CHALMERS
UNIVERSITY OF TECHNOLOGY

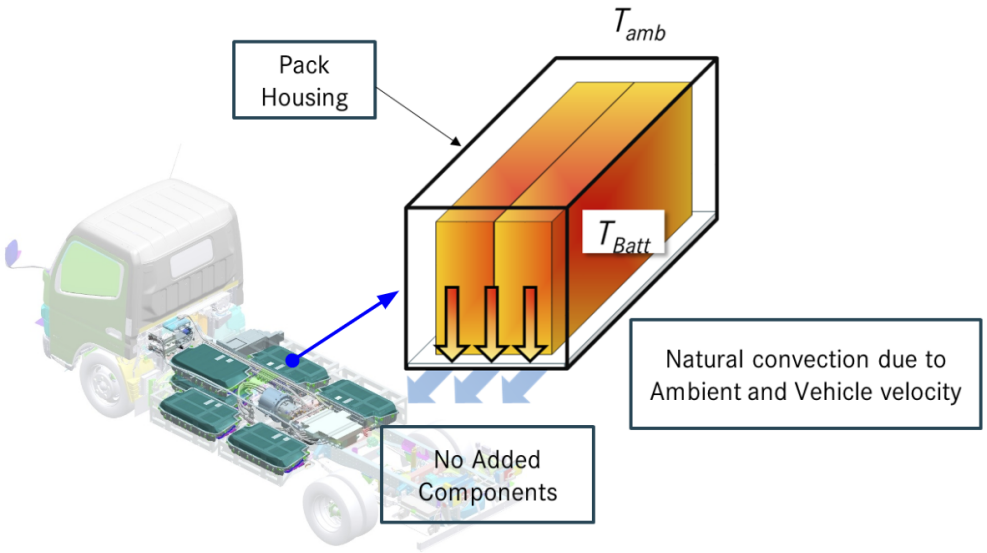

Performance and Feasibility Evaluation of Passive Battery Cooling System in Electric Trucks

Electro-thermal simulations of the HV Battery

Master of Science Thesis

AADITHYA GANESH

Department of Energy and Environment
CHALMERS UNIVERSITY OF TECHNOLOGY
Gothenburg, Sweden 2019

Master's thesis 2019

Performance and Feasibility Evaluation of Passive Battery Cooling System in Electric Trucks

Electro-thermal simulations of the HV Battery

AADITHYA GANESH

CHALMERS
UNIVERSITY OF TECHNOLOGY

Department of Energy and Environment
Division of Electric Power Engineering
Chalmers University of Technology
Gothenburg, Sweden 2019

Performance and Feasibility Evaluation of Passive Battery Cooling System in Electric Trucks
AADITHYA GANESH

Supervisors: Dr. Vikram Menon, Daimler Trucks Asia
Simon Oberhoffer, Daimler Trucks Asia
Examiner: Dr. Torbjörn Thiringer, Department of Electric Power Engineering

Master's Thesis 2019
Department of Energy and Environment
Division of Electric Power Engineering
Chalmers University of Technology
SE-412 96 Gothenburg
Telephone +46 31 772 1000

Cover: A passively cooled HV battery pack of an electric Light Duty Truck (LDT).

Performance and Feasibility Evaluation of Passive Battery Cooling System in Electric Trucks
AADITHYA GANESH
Department of Energy and Environment
Division of Electric Power Engineering
Chalmers University of Technology

Abstract

The E-mobility trend is catching up in the commercial vehicle segment and one of the major challenges in this topic is the thermal management of the Li-ion HV battery. The thermal management system typically comprises of forced liquid cooling also known as active cooling system which maintains the battery in a safe operating temperature range. This function helps to obtain maximum electrical and chemical performance from the battery cells, required for an hassle-free propulsion. The key point of interest for engineers is reducing the complexity of the thermal management system which would in turn reduce the weight and energy consumption of the HV battery and lead to an increased driving range. Recently, passive cooling has been considered as sufficient and has been proven to be a replacement for active cooling in certain electric vehicles. In this thesis, a passive cooling system and an active cooling system are set up for the HV battery of an electric light duty truck (LDT). Electro-thermal simulations carried out using MATLAB (Simulink) are capable of computing residual heat and in turn predict the battery temperatures for various discharging and charging load cases. A weighted point algorithm is introduced to compare and analyse the passively cooled battery with its actively cooled counterpart in terms of feasibility and performance for various market locations. It was found that passively cooled batteries are suitable for all market regions lying in the ambient temperature range of 0-15°C. It is also recommended that passively cooled batteries can replace the actively cooled batteries for customers driving in city regions located in the temperature range of 0-30°C. Passive cooling is an economical and practical solution since it was found to extend the LDT's vehicle range by 5km and also reduced the battery system cost by 11%.

Keywords: Electric trucks, HV Battery simulation model, Passive cooling system, Thermal Management System, Weighted point algorithm, Thermal states, lumped electro-thermal representation for HV battery

Acknowledgements

This master's thesis project was conducted in Daimler Trucks Asia, Japan during spring 2019. Firstly, I would like to thank my examiner Dr. Torbjörn Thiringer and the department of Electric Power Engineering at Chalmers University of Technology for their encouragement in letting me pursue my thesis in Japan.

I would like to thank my supervisors Dr. Vikram Menon and Simon Oberhoffer for their constant guidance and support. Regular project reviews and feedback meetings with my examiner and supervisors helped me to acquire the needed skills and knowledge in battery development.

I'm also grateful to Deepak Raut and Dr. Isais Oliva for their fruitful discussions and constructive feedbacks. Special thanks to my colleagues Watauchi Naoki and Koda Naoki for kindly supporting me to learn the Japanese language and understand their culture. It made this project even more interesting and a special event in my Master's journey.

Finally, I would like to thank my family and friends for their love and care throughout.

Aadithya Ganesh, Gothenburg, December 2019

Contents

1
Introduction

This chapter presents a brief overview of the topics discussed in the various sections of this thesis.

1.1 Background

Over the years, transportation industry has been one of the major contributors of global emissions and energy consumption. Concerns have been risen regarding the usage of the internal combustion engine (ICE) vehicles and has led to the introduction of fully electric vehicles (EVs), Hybrid vehicles (HEVs) and fuel cell electric vehicles (FCEVs) [1]. The source for propulsion in these new generation of vehicles is high voltage battery. The requirement of large electric power for these vehicles led to the introduction of Lithium (Li) ion batteries as a replacement to the previously used lead acid battery.

Li ion batteries generate heat due to rapidly changing charging and discharging cycles that they are exposed to during vehicle acceleration and deceleration [1].The heat generated in a Li-ion battery cell is mainly due to the entropy change occouring from electro-chemical reaction and ohmic heating caused by the internal resistance of the cell [2]. This phenomenon is quite a concern for the engineers since it largely influences the lifetime and performance of the battery packs. In general the thermal management system for the batteries of EV/HEV's are required to maintain the battery temperature between 25 and 40^oC. It is also important to maintain uniform temperature across the whole pack by maintaining the mean cell temperature distribution below 5^oC [1].

If the above stated situations are not achieved, then the thermal issue directly affects the electro-chemical system, round trip efficiency (i.e) the fraction of energy that could be put into or retrieved from a battery, power and energy capability, reliability, cycle life and cost. A Battery Thermal Management System (BTMS) consists of two components namely the cooling System and cooling strategy. A particular vehicle application containing a HV battery with a particular cell chemistry requires a certain BTMS [3]. Performance evaluation of the BTMS is necessary for the selection process and it mainly involves the study and comparison of a charging and discharging battery temperature profile and mean cell temperature distribution. Further, interesting parameters include the effective vehicle range, energy consumption of the BTMS, estimated cost and weight added to the e-powertrain. The e-powertrain of

the Light Duty Truck (LDT) is much bigger compared to that of a passenger car. The electric LDT is designed to carry 1-4 ton as payload. Typically, it is used as a delivery vehicle and is expected to provide 100km range for one complete discharge cycle of the battery. Recently, automotive manufacturers have shown interest in producing electric vehicles without any BTMS. Battery packs without any "active" cooling components are called passively cooled battery packs. This has attracted interest since, we could increase driving mileage by reducing the weight and energy consumption of the battery.

1.2 Objectives

The objective of this master thesis is to identify the possibility of passively cooled HV batteries in electric trucks. Performance analysis was carried out against actively cooled counterparts, in order to identify the feasible customers and market regions that are suitable for adapting passively cooled batteries.

1.3 Limitations

The simulation model in MATLAB Simulink considers the following assumptions and limitiaions:

- The Li-battery used considers the Nickel Manganese Cobalt Oxide (NMC) Li-ion cell chemistry typically used in Parallel Plug-in Hybrid Electric Vehicle (PHEVs), which require high power output capabilities.
- The passive cooling model for battery doesn't consider the variation in heat transfer across different packs placed in different locations in the powertrain.
- The battery is always considered in beginning of life (BOL) and the capacity loss prediction due ageing of the cells is not considered.
- Calendar and cyclic ageing models of the cells are not used in this thesis and has to be added further to the simulation model in order to make the results very realistic.
- This simulation shall not consider any preconditioning of battery before usage in the vehicle.
- It also doesn't account for unequal current distribution due to a variation in string impedance, which in reality leads to unequal module temperature.

2
Theory

2.1 Electric Commercial Vehicle

The commercial vehicle segment has slowly gained momentum to catch up with the e-mobility trend. The major classification in the commercial trucks segment are Light, Medium and Heavy duty. The first step towards the trend begins with electrification of light duty trucks (LDT). Table 2.1 presents the LDT's information discussed in this thesis.

Table 2.1: Specification of electric light duty truck

Total vehicle weight	7.5 ton
Payload	1- 4 ton
Speed	80-105 km/hr
Gradability	12-20%
Range	100 km
Charging time	1-2 hrs
Power peak/cont.	100/45 kW

The major motivation for electric LDT are based on various political, social, economical and technological benefits. Legislative frameworks of the EU for example, have CO_2 based taxes for M1 and N1 classes of vehicles which add up as Annual Circulation Taxes (ACT) [11]. These strong restrictions have influenced the Light Duty Truck (LDT) to turn fully electric, after passenger cars. Compared to an electric passenger car, the LDT requires a bigger battery pack in order to meet its load and duty. A single HV battery pack used in this electric LDT has the specification shown in Table 2.2. The truck which is discussed in this thesis requires six of these battery packs in series. Together, they could store $82.8kWh$ of energy at a maximum DC voltage of $420V$.

Table 2.2: Specification of HV battery

Norm./ Max. voltage	365/420 V
Capacity	37.5 Ah
Energy	13.8 kWh

The HV battery could be charged by both AC and DC modes of charging. It mainly supports a $115kW$ electric motor with a maximum torque of $390Nm$. It contains

Nickle-Manganese-Cobalt (NMC) Li-ion cells. The operation and performance of these Li-ion batteries depend on its electro- chemical properties, variation in ambient temperature and their charging and discharging load cycles.

Passively cooled HV batteries are gaining popularity in electric vehicles and there is a possibility that they might replace actively cooled batteries. The major drawback with passively cooled batteries is that, they can not be heated up or cooled down at any desired instant. We would solely, depend upon the load of the battery for heating up and the ambient conditions for cooling down. Regardless, it drew attention when Nissan introduced the new Leaf with a passively cooled HV battery. As soon as it worked, the idea was further carried over to their commercial van, Nissan e-NV200 [12]. Their vehicles are limited to certain conditions based on their customer application and the nature of their target market. Volkswagen built a race car with passively cooled batteries to conquer the Pikes peak. The fundamental goal was to reduce the drive train weight and utilise the aerodynamics to cool the battery instead of using active cooling [13]. This inspired us to investigate, if there is a possibility for adapting passively cooled HV batteries in electric trucks.

2.1.1 Temperature profiles in market regions

The feasibility of electric vehicles are largely influenced by the ambient conditions that the HV battery is subjected to. Typically, the actively cooled batteries are isolated from the atmosphere by a moulded plastic housing of high thermal capacity. In such cases, the battery temperature is only influenced by the operation of the active cooling components. But, in case of a passively cooled battery, the ambient temperature majorly influences the battery temperature since, the module surface is directly in contact with the environment.

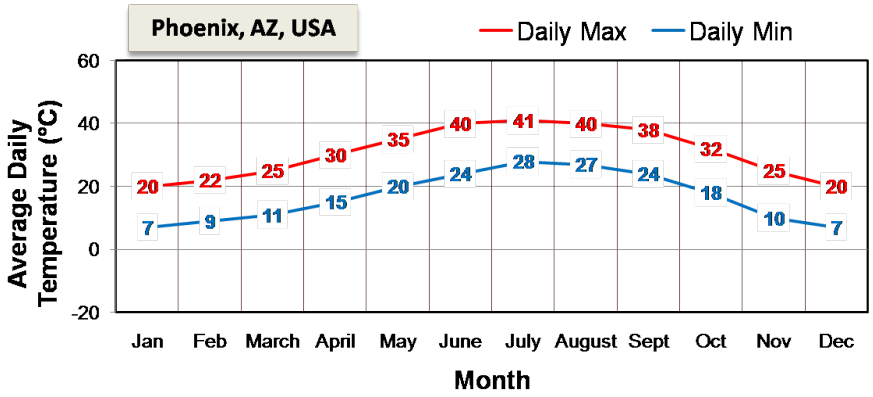

Figure 2.1: Average monthly temperature distribution in a hot market region

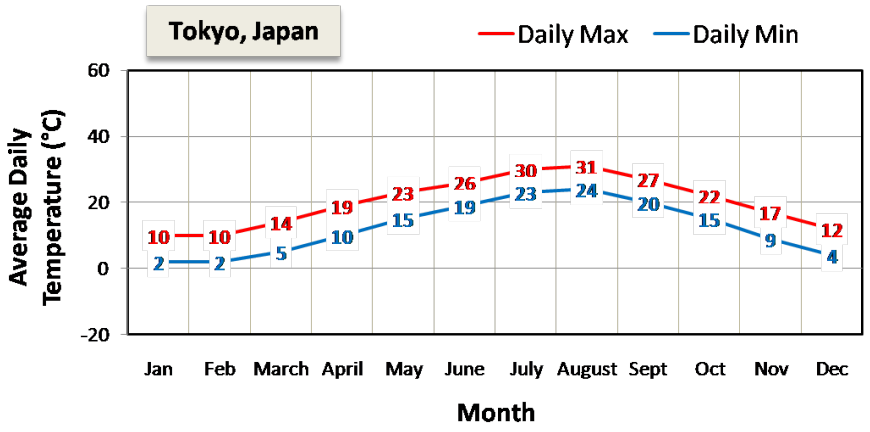

Figure 2.2: Average monthly temperature distribution in a moderate market region

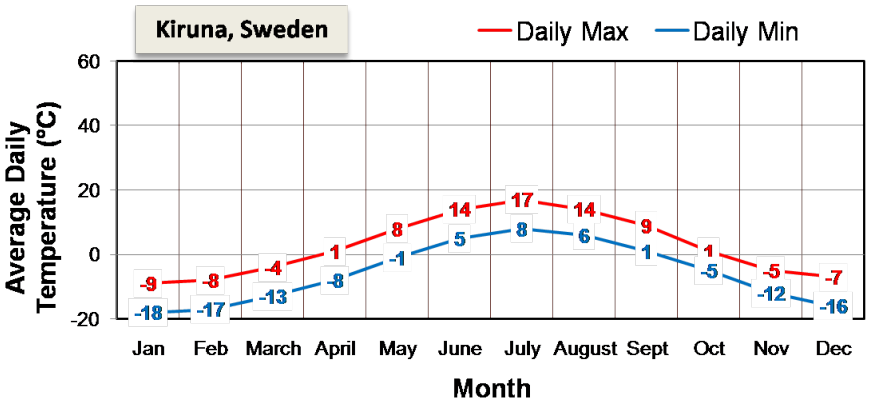

Figure 2.3: Average monthly temperature distribution in a cold market region

The average monthly temperature distribution for hot, moderate, cold market regions are shown in figures (2.1), (2.2), (2.3). Phoenix, Arizona in USA is an example of a hot market region since, it is generally warm and especially during summer, the temperature could reach an average maximum of 41°C. Tokyo, in Japan is an example for moderate market region whose average daily temperature variation is neither too hot nor too cold. Kiruna in Sweden, is a good example of a cold market region because the average daily temperature is sub zero for almost 7-8 months of the year. On the coldest day, the temperature would reach an average minimum, as low as -18°C.

These ambient temperature variation data gives us the idea of initial battery temperature, that we could assign for our simulations. Hence the graphs could be summarised to be distributed between -20°C till 50°C. This would include extreme ambient temperature conditions and in turn would help us to estimate the working boundaries for the passively cooled batteries.

2.1.2 Load Cycles for the battery

The basic operation of an electric truck by means of discharging and charging of the HV battery is majorly responsible for the battery temperature. Original equipment manufacturers (OEM) generally use customer usage profiles and some other standard drive cycles for the HV battery design and development. These cycles are considered as load cycles to the HV battery and they are useful for verifying the electrical and thermal safety limits during real time operation.

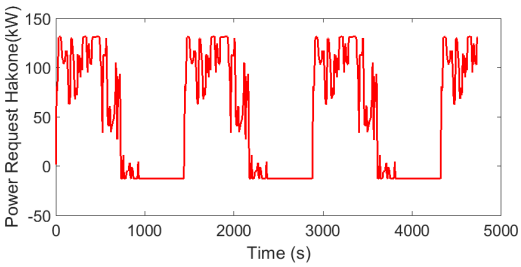

Figure 2.4: Rural drive cycle load

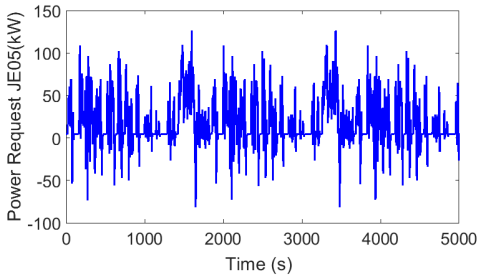

Figure 2.5: Urban drive cycle load

As a first step, it is common to use a case where the HV battery's thermal safety limits could be crossed. To simulate this extreme condition, a rural customer drive cycle is chosen. It is basically a condition where the customer is climbing the mountain Hakone in Japan, trying to maintain a constant truck speed of $50km/h$. The variation in elevation requests for electric power from the HV battery system as shown in fig.2.4. The average discharging C rate of this load cycle for one out of the six HV batteries is $0.6C$.

The second drive cycle chosen is an urban drive cycle. It is called the JE05 drive cycle and its profile corresponds to the scenario when the LDT is driven in the city of Tokyo, Japan. It is one among the approved homologation standard drive cycles for electric light duty trucks in Japan. When compared to Hakone, JE05 is a less severe drive cycle and discharges one battery pack at a $0.2C$ discharge rate. The power request profile of this urban drive cycle is shown in figure 2.5.

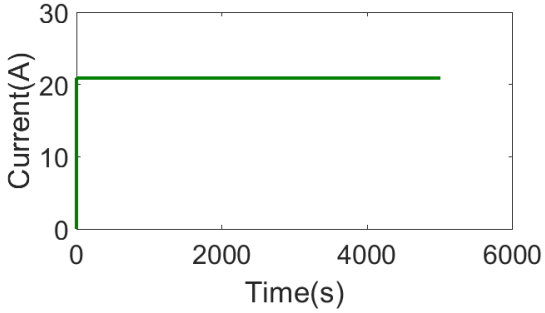

Figure 2.6: DC charging current load

The final load cycle which affects the battery temperature is the charging scenario. The current profile of 50kW DC charging is represented in figure 2.6. DC charging is chosen here instead of AC charging since, it is also a severe load cycle like the rural discharge cycle. The $7.7kW$ and $22kW$ AC charging don't influence the battery temperature as much as the DC fast charging. With the DC condition, the pack is charged at a $0.55C$ rate. Also, it is important to note that, in all of these conditions the rated capacity of a pack is $37.5Ah$. More analysis methods of battery operation using real life load cycles based on its the duty cycle eccentricity (DCE) is discussed in [6].

2.2 Features and Characteristics of High Voltage Battery

2.2.1 Li-ion battery

Initially lead acid batteries were used in Internal Combustion Engine(ICE) vehicles for ignition and other auxiliary purposes. With time, this was carried over to Electric Vehicles(EV) functioning as HV battery source because they were cheap. However lately, they have been ruled out due to their low energy density. Subsequently, the technology in EV variants evolved into Li-ion batteries. This technology was well accepted because of its compatibility with the high voltage platform, high energy density, low self discharge rate and longer cycle life performance.

Parameters of Li-ion battery like charging/ discharging current, voltage, cell operation temperature are continuously monitored using control electronics, referred to as Battery Management System (BMS). The non-linearity associated with Li-ion battery operation could be attributed to the variation in internal resistance (R_i) with respect to its state of charge(SOC) and temperature. Apart from the BMS, the HV batteries in EVs also require their cells to be operated within a safe operating temperature range, ideally between 25 to 35^{o}C. This is performed by a Battery Thermal Management System (BTMS) which consists of a suitable cooling system and cooling strategy for the battery. The subsequent sections compare three different Li-ion cell chemistries based on their characteristics and properties.

2.2.2 Energy and Power requirements from HV battery

The choice of cell chemistries for a HV Battery of any electric vehicle depends on the specific energy and power requirements. The need varies with respect to vehicle application, charging time, discharge power requirement and vehicle range between two charging events. However, the common goal and requirement in all newly developed cell chemistries remain the same, i.e to to achieve a long life. The characteristics and properties of the different cells compared here could be broadly classified based on their specific energy (in Wh/kg), power (in W/kg), battery safety, discharging and charging performance, life span (ageing of cells) and cost.

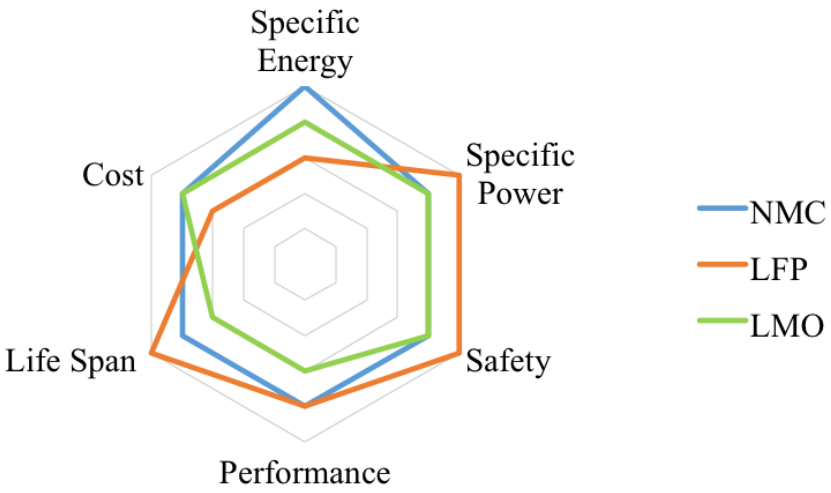

Figure 2.7: Comparison of different Li-ion cell chemistries

Figure 2.7 shows the comparison of popularly known Li-ion cell chemistries, like $LiNiMnCoO_2$ (NMC), $LiFePO_4$ (LFP) and $LiMn_2O_4$ (LMO). The chart presented is based on the data mentioned in [10]. The greater the area covered in the spider chart, the better is the performance of that particular cell chemistry. Functionally, the commercial EVs require a HV battery with high capacity (specific energy) and high specific power (maximum load current) for full filling vehicle requirements and also in order to obtain lighter battery packs.

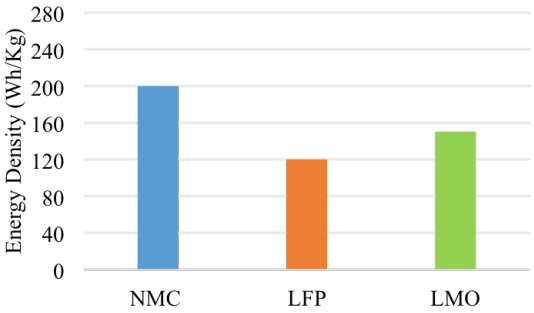

Figure 2.8: Energy Density of different Li-ion cell chemistry

Figure 2.8 compares energy density(Wh/Kg) of different Li-ion cell chemistries. An NMC electrode in Li-ion batteries will have the highest energy density, followed by LMO and then LFP. The manganese present in LMO cells, form a three-dimensional spinel structure that improves ion flow, reduces internal resistance and in turn improves its current handling capabilities [9]. However, it offers suffers from a short life span which further demanded researchers to explore better chemistries for practical viability. The LFP chemistry on the other hand, has higher specific power (maximum current rating) and longer life span. It also has a wide operating temperature range, lying between -30°C and 60°C [9]. But, in order to overcome its higher self discharge rate, the battery development cost is quite expensive. The NMC chem-

istry in Li-ion batteries are designed to provide high specific energy or power. It is the most commercially successful Li-ion cell solution for EV till date. The secret lies in the combination of Ni and Mn, which produces high specific energy/power and low internal resistance [9] [10]. This makes them suitable for large scale production of HV batteries required for this EV application.

If the above parameters are not taken into account for the cell chemistry selection in a HV battery, then it leads to a mismatch and would result in a poor performance. Consequently, there would be wearing of the battery during each cycle and it would cause unexpected heating. Additionally, the battery would then require special resources for maintenance.

2.2.3 Safe Operating Area (SOA) of Li-ion battery

For Li-ion batteries, the safe operating area (SOA) could be defined as the voltage, current and temperature limits within which it can operate without any self damage. The battery management system (BMS) monitors and operates the battery within its electrical limits. Similarly the battery thermal management system (BTMS) is responsible for operating the battery within its limited safe operating temperature. The electrical and thermal safe operating area is specified by the cell supplier and it is the responsibility of the OEM to analyse and understand this before it is used in the electric vehicle application.

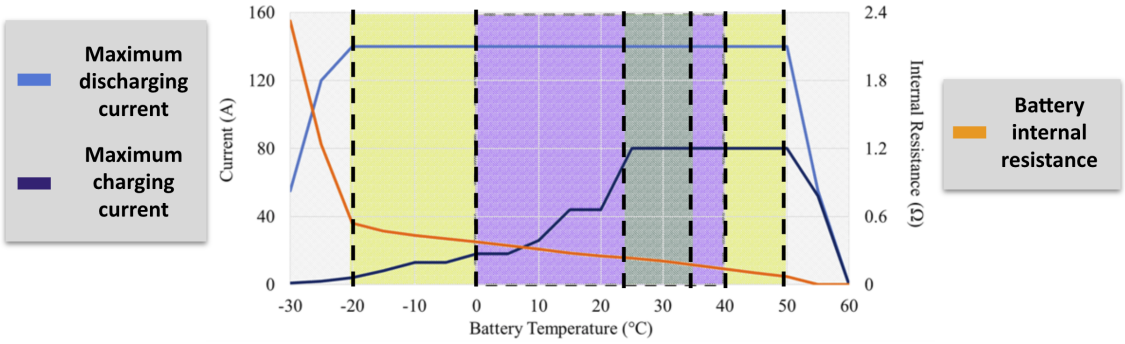

Figure 2.9: NMC Li-ion battery characteristic profile

The NMC Li-ion battery pack's maximum continuous charging, discharging current and the internal resistance are plotted as a function of battery operational temperature in figure 2.9. This area under the temperature range, -20°C and 50°C is called as thermally safe operating area. The data of this characteristic profile corresponds to the battery pack's s-function explained in the simulation set-up later in this thesis. The optimum operational temperature range for Li-ion battery pack, represented by the shaded green region is between 25°C and 35°C. However, it is practically not possible to always operate the battery within this optimum temperature range because it is very narrow and it would require a complex BMS and BTMS. The installed control mechanisms would consume a lot of energy from the battery. Hence, there is a compromised temperature region which is between optimum and the safe

operating area of the battery pack. This is usually the temperature limit for the practical thermal management control system and hence it suitably called as the control temperature region. It lies between 0°C to 40°C and is represented by the shaded purple region.

A battery temperature below 0°C, is not preferred because the viscosity of the electrolyte increases, thereby reducing the ionic conductivity. This is responsible for the steep increase in internal resistance in the low temperature region. Additionally, since the charge transfer resistance of a discharged battery is much higher than that of a charged battery. It is quite difficult to charge the battery at very low temperatures. Another challenge for charging at low temperature is the condition called Li-plating. The Li-ion intercalation into the anode from the cathode is slowed down due to its polarization. These ions deposit on the surface of the electrode and subsequently reduce the battery capacity. Hence, the maximum charging current is highly limited for battery temperature below 0°C.

Similarly there are degrading effects in the battery at high temperatures. The usage of a battery at a temperature above 40°C, causes loss in capacity and accelerated ageing. Further, for a temperature above 50°C, the maximum charging and discharging currents are restricted due to the fear of thermal runaway condition. High temperature triggers uncontrollable exothermic reactions which could lead to a fire or an explosion. More details about temperature effects on Li-ion battery's performance could be found in [8].

2.3 Electro-Thermal Relationship in Li-ion battery

2.3.1 Heat Generation in Li-ion cell

The heat generation occurring inside the cells of the battery, are due to electrochemical reactions occurring during charge transfer and due to ohmic losses occurring in the components of the battery during charging and discharging events. They can be written using the following expressions,

$$\begin{aligned} \dot{Q}_{Gen} &= \dot{Q}_r + \dot{Q}_{irr} \\ \dot{Q}_r &= IT\frac{dU_{OCV}}{dT} \\ \dot{Q}_{irr} &= I(V - U_{OCV}) = I^2 R_i \end{aligned} \tag{2.1}$$

The first term in (2.1), $\dot{Q}_r$ represents the reversible heat generated in the cell, dU_{OCV}/dT is the entropy coefficient of the reversible process, U_{OCV} is the open circuit voltage of the cell. The second term $\dot{Q_{irr}}$ represents the irreversible heat generated due to polarisation of the cell. It is represented by $I(V - U_{OCV})$, where I is cell current, V is cell voltage. Further, it can also be electrically represented as ohmic heat, I^2R_i. Here, R_i represents the cell internal resistance. Typically, the

irreversible heat generated is greater than the reversible heat generated for practical EV loads.

2.3.2 Modes of Heat Transfer

The heat generated due to charging and discharging events of the battery has to be removed by some means. Else, the stored heat in the battery would increase the cell temperatures. For maintenance of the battery temperature within a desired range, sufficient heat needs to be removed in the case of a hot ambient condition or must be added in the case of a cold ambient condition. This is executed using three fundamental heat transfer phenomena called as conduction, convection and radiation. Mathematically, the general expressions representing these modes of heat transfer are shown below,

$$\begin{aligned} \dot{Q}_{sink} &= \dot{Q}_{cond} + \dot{Q}_{conv} + \dot{Q}_{rad} \\ \dot{Q}_{cond} &= \frac{\lambda}{d} A(T_1 - T_2) \\ \dot{Q}_{conv} &= h(Re, Nu, Pr) A(T_{Batt} - T_{med}) \\ \dot{Q}_{rad} &= \epsilon \sigma A(T_{Batt}^4 - T_{med}^4) \end{aligned} \tag{2.2}$$

Heat transfer due to conduction takes place in all mechanical connections of the cell surface. In the expression (2.2), λ is the thermal conductivity of the material, d is the thickness of the surface in contact with the heat source object and $T_1 - T_2$ is the temperature difference between the two conducting solid surfaces.

The second mode of heat transfer is convection. This could be further classified as natural and forced convection based on weather the cooling media is actively driven by certain mechanism or is naturally cooling the source object. The convective heat transfer co-efficient is denoted as h, which is a function of Reynolds, Nusselt and Prandtl's number of fluid flow. Convection is also a function of contact surface area, A and the temperature difference between the media.

Finally, heat transfer due to radiation is represented by the Stefan-Boltzmann equation. ϵ is called as the emission co-efficient of the source material and σ is known as the Stefan-Boltzmann constant whose value is $5.670310^{-8}(W/m^2K^4)$. Similar to conduction and convection, radiation is also a function of surface are of the source object and the temperature difference between the separating media.

These fundamental expressions of heat generation and heat transfer help us to track the flow of heat flux from cell to cooling medium. Brief explanation for the above equations and constants could be found in [3].

2.4 Cooling System for a HV battery

2.4.1 Active cooling system

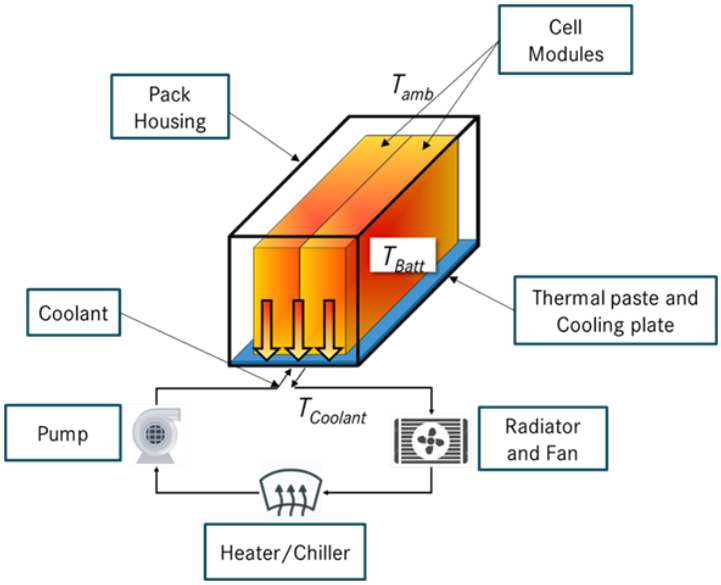

Figure 2.10: Active Cooling of HV battery

As discussed before and schematically shown in fig. 2.10, the active cooling system of a HV battery contains cooling plates with ethylene-glycol and water coolant pumped in and out through tubes contained inside the cooling plate. The active components like fan, heater and chiller which control the rate of heat transfer are parts of the same circuit and they consume electrical energy from the same HV battery for their operation. Further, there is another active cooling system present separately for the electric motor which is powered by the low voltage (LV) battery. It can be considered as a different cooling circuit and the coolant typically used is oil.

Even though there are so many coolants available, the most popularly used one is the ethylene glycol water mixture. It is preferred because of its anti-freeze property until -35°C, which includes the minimum allowed battery operation temperature of -20°C. It requires a flowrate of $6LPM$ in the cooling circuit to achieve efficient cooling. Usually, the coolant is initially pumped at a temperature, 2° lower than the battery temperature. Then the active components are switched ON to either add or remove heat to the coolant in order to control the battery temperature within a specific range. Also, the rate of adding or removing heat is governed by the switching of these active components.

2.4.2 Passive cooling system

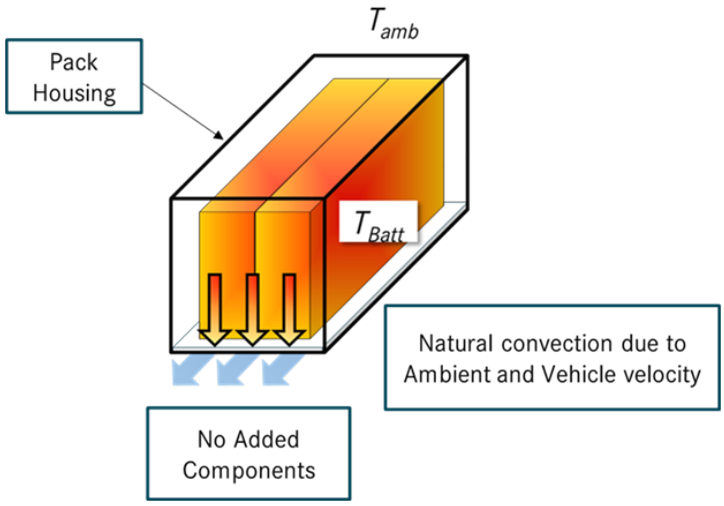

Figure 2.11: Passive Cooling of HV battery

Passive cooling of the HV battery is done only through natural or forced convection using ambient air as coolant. As shown in fig. 2.11, there are either no active components or just minimum active components, like only a fan would be attached to improve the air flowrate across the surface of the cooling plate. The coolant here is ambient air and no other liquid coolants are used. The heat flux originates inside the cell due to electro-chemical reactions as discussed in the previous section and its direction of flow is represented by the red-yellow arrows. It is conducted effectively to the cooling plate via the thermal paste, since the effective thermal resistance along this path is maintained minimum. The surface area for cooling is now increased because of the cooling plate and the heat is either removed or added using convection. The heat transfer now depends on temperature difference between the cells and the atmosphere and also on the flow rate of air. The rate of cooling is improved with an increase in vehicle velocity. Also, there has been a large interest to increase the heat transfer coefficient by introducing suitable cooling fins on the surface of the cooling plate, similar to the cooling of semiconductors in modern computers.

Since, the active system for cooling and heating of the HV battery has been established as a good solution, engineers now wish to take a step back and would like to analyse the possibility of the passive system and other modern techniques.

2.4.3 Contemporary and Developing cooling methods

Ethylene glycol water cooling system is the most commonly used liquid cooling for a HV battery. Another liquid that is preferred over the years is oil cooling, but it is not practical for large HV battery pack because of their density. Now, researchers have come up with nanofluids where Al_2O_3 or carbon nanotubes are suspended in water. These nanofluids are known for their high thermal conductivity. Phase changing materials are also catching up in cooling applications. Gallium metal, phase changes

from solid to liquid at room temperature and works as liquid coolant. Even though its cooling performance is better than water, it is not practically viable since it requires special electromagnetic pumps for transportation. Similarly, there are liquids with a boiling point of 35°C which is close to the ideal Li-ion battery temperature. They are currently available in the market called as Novec 7000 produced by 3M. Also there are other heating solutions available for the battery, when it operated in low temperatures. For example, there is a mutual pulse heating method, which uses forced discharge pulses to increase the battery temperature. More details about these developing cooling and heating solutions could be found in [7], [20], [21].

2.5 Lumped Thermal Network Representation

The physical process of heat generation and transfer using active or passive cooling can be represented through the lumped thermal network. The basic ideology is to treat the system as a combination of resistances and capacitances. The thermal correspondence to electrical parameters, which is useful for setting up the lumped thermal network are presented in table 2.3.

Table 2.3: Electrical relation of thermal quantities

Electrical	Thermal
Voltage (V)	Temperature (T)
Current (I)	Heat flux ($\dot{Q}$)
Resistance (R)	Thermal resistance (R_{th})
Capacitance (C)	Thermal capacitance (C_{th})

This lumped thermal network representation would help us to determine the instantaneous thermal parameter values of a HV battery and its cooling system.

$$V(t) = IR(1 - e^{\frac{-t}{RC}}) \tag{2.3}$$

In electricity, the potential difference at any instant $V(t)$, across an RC electrical circuit is given by (2.3). Here, I is the current through the circuit and t is the time.

$$T(t) = \dot{Q}R_{th}(1 - e^{\frac{-t}{R_{th}C_{th}}}) \tag{2.4}$$

Similarly, in a thermal RC network representation the temperature difference at any instant, $T(t)$ between the source and the node of study is given by the relation (2.4).

$$\begin{aligned} R_{th,cond} &= \frac{d}{\lambda A} \\ R_{th,conv} &= \frac{1}{hA} \\ C_{th} &= C_p M \end{aligned} \tag{2.5}$$

With the values obtained for R_{th} and C_{th}, the temperature at different locations in the battery pack could be found out for a known value of heat flux. As shown in (2.5), $R_{th,cond}$ is the thermal resistance due to conduction, d is the thickness of the

object, λ is the thermal conductivity and A is the surface area. Similarly, $R_{th,conv}$ is the thermal resistance due to convection and h is the convective heat transfer coefficient. The thermal resistance due to radiation is not considered in a a lumped thermal representation, since its value is insignificant in batteries. Finally, C_{th} is the thermal capacitance which is the product of heat capacity, C_p and mass of the object M.

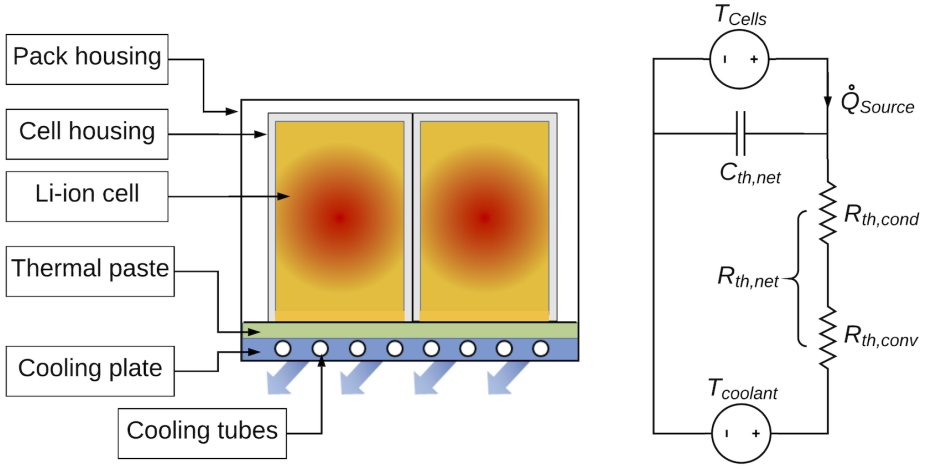

Figure 2.12: Lumped thermal network of HV battery and its cooling system

The physical components of the Li-ion battery and its simplified lumped thermal network is shown in figure A.6. In an actively cooled HV battery, the coolant is ethylene glycol-water mixture. Hence, its derived thermal parameters are represented in the Table 2.5.

Table 2.4: Thermal quantities of an actively cooled battery

$C_{th,net}$	112,000 (J/K)
$R_{th,cond}$	2 (K/kW)
$R_{th,conv}$	24 (K/kW)

Similarly, the network parameters for a passively cooled battery is presented in the Table 2.5.

Table 2.5: Thermal quantities of a passively cooled battery

$C_{th,net}$	112,000 (J/K)
$R_{th,cond}$	2 (K/kW)
$R_{th,conv}$	231 (K/kW)

More applications of lumped thermal representation for analysing the battery temperature is discussed in [16], [17]. A brief explanation regarding the derivation of lumped thermal network parameters for this particular HV battery is given in Appendix A (A.1.2).

3

Case Setup

3.1 Flow chart of Case setup

The steps to be followed in order to set up passive cooling for an electric LDT's battery and compare its performance and feasibility with respect to active cooling is shown in figure 3.1.

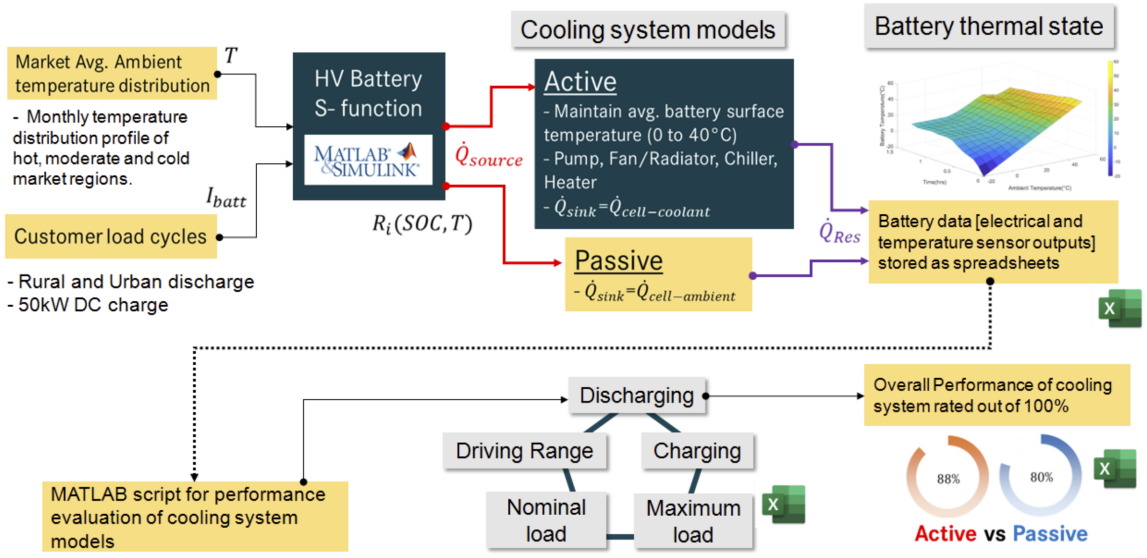

Figure 3.1: Process involved in performance simulations

Firstly, we shall begin by defining the inputs required for battery simulations. The HV battery s-function implemented in Simulink, MATLAB requires the battery temperature and the current as inputs. This is obtained using the average ambient temperature distribution and the customer load cycles (consisting of rural and urban discharging and 50kW DC charging cycles). The NMC Li-ion battery pack implemented as a s-function in Simulink, MATLAB contains its electro- thermal properties. The heat generation and heat loss modelled in the s-function is based on the internal resistance data for this NMC battery pack, provided by the supplier. The internal resistance is a function of state of charge (SOC) and battery temperature.

The subsequent step is the integration of active and passive cooling system models to the HV battery s-function. The active cooling system consists of pump,

fan/radiator, chiller and heater models to modify the coolant inlet temperature and flowrate. The active cooling system model calculates the heat lost from the cells to the coolant, $\dot{Q}_{Cell-Coolant}$. Similarly the developed passive cooling system, calculates the heat lost from the cells to the ambient, $\dot{Q}_{Cell-Ambient}$. The difference between the heat generated from the cells, $\dot{Q}_{source}$ and the heat lost to the cooling system, $\dot{Q}_{sink}$ gives the residual heat remaining in the battery pack, $\dot{Q}_{residual}$. This is responsible for the rise or drop in battery surface temperature that is obtained through these simulations. The simulation output data are exported and stored in Microsoft Excel.

This data is analysed using a performance evaluation script written in MATLAB, which is called as the weighted point algorithm. The logic and working of this algorithm is explained later in this chapter. The output analysis report is written in Microsoft Excel, as a spider chart. The chart contains Discharging, Charging, Maximum load, Nominal load and Driving range as its performance parameters. From the results, the feasibility rating of the cooling systems could also be obtained, and it is also indicated in figure 3.1.

Finally, it is required to validate the base simulation model, which is the HV battery and active cooling system. Then, it is required to verify the heat transfer modelled for passive cooling using the values found in literature. The battery temperature with active cooling is validated using the data recorded from actual test vehicle. These results are presented and discussed in the next chapter.

3.2 HV Battery simulation model

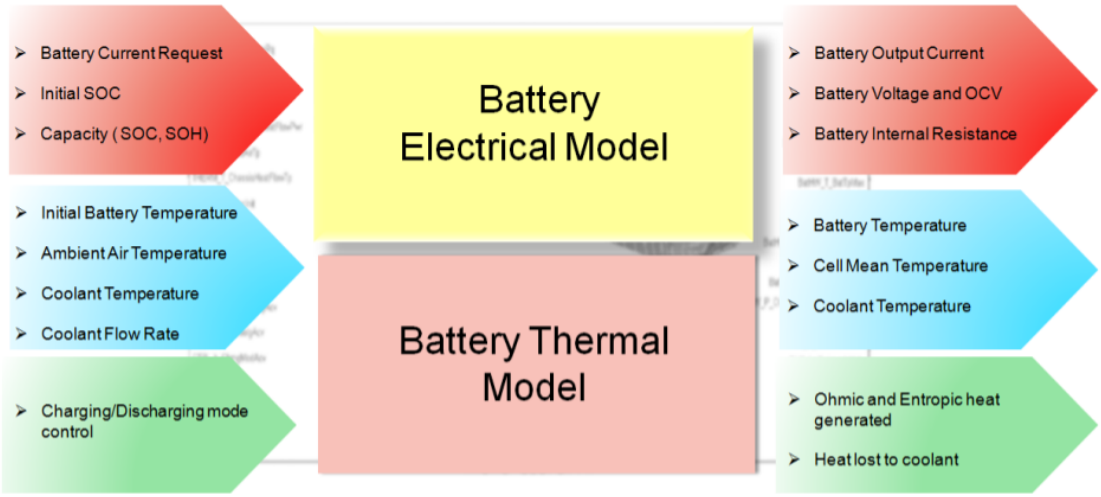

Figure 3.2: HV Battery function in Simulink

Figure 3.2 shows the various input and output features of the HV battery s-function in MATLAB. The electrical inputs firstly contain, the battery current which can be fed as either charging or discharging. It is decided based on whether the current

direction to the battery is either positive or negative. Then, there is a feature available to define the initial state of charge and health (SOC and SOH). This would determine the internal resistance offered by the battery pack for the user specified conditions.

The s-function contains the NMC Li-ion battery pack with the functions for the liquid cooling. The physical appearance of this pack is shown in figure 2.10. The temperature dependence of this battery's parameters is represented in figure 2.9. This brings us to our second set of inputs, which are the initial battery, ambient air and coolant inlet temperature. These are required to define the initial thermal state of the system. The coolant flowrate through the pipes of the cooling plate in the case of actively cooled battery, could be defined between 0-6 litres per minute (LPM). Finally, there is a control input to indicate charging or discharging mode of the battery.

The output gives the next electrical and thermal states of the battery. Also, it gives the ohmic and entropic heat generated and the heat lost to the coolant. This information is very useful to design the cooling system model and thermal management control strategy. For the case of a passive cooling system, this s-function can't be directly used, rather a work around has to be made for it to act as if there is no coolant and the battery is simply cooled by the atmosphere. The cooling system models implemented in simulations are shown in the next section.

More details regarding the battery s-function modelling is discussed in Appendix A. The recreation of battery behaviour in a simulation requires a lot of data containing its electrical and thermal parameters. These values can only be obtained by carrying out experiments. More details could be found in [25], [26], [27] and [28].

3.3 Cooling System Model

The active and passive cooling system Simulink models for the LDT's HV battery are shown in figure 3.3. The selection of the type of cooling system, type of load and initial conditions for the battery simulations are called from a separate script in MATLAB.

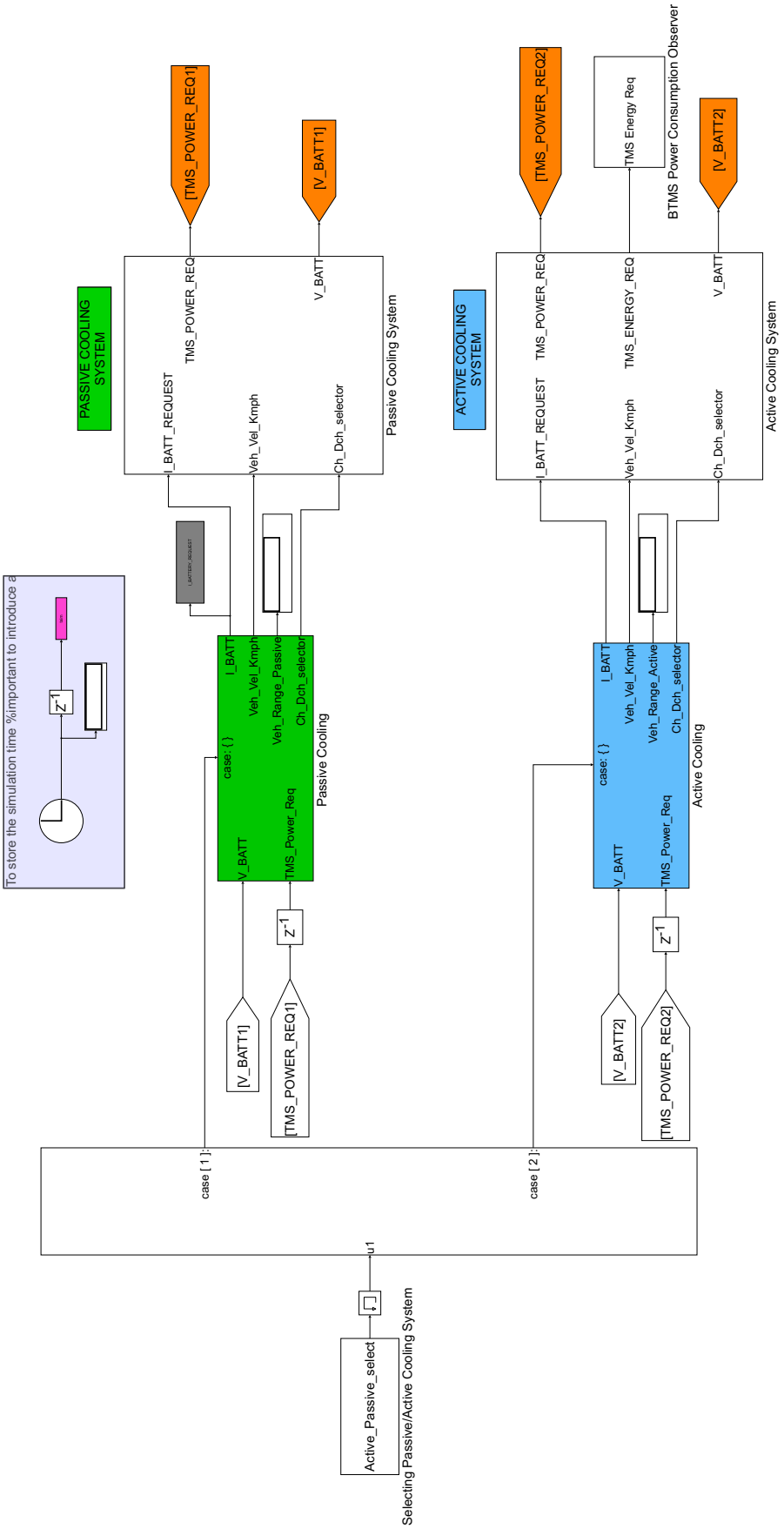

Figure 3.3: Cooling system models in Simulink

3.3.1 Thermal management strategy

The thermal management strategy is the decision maker, which controls the switching of the active components shown in fig. 3.5. Detailed descriptions regarding the modelling of the active cooling components such as chiller, heater, pump, radiator and fan are given in [7].

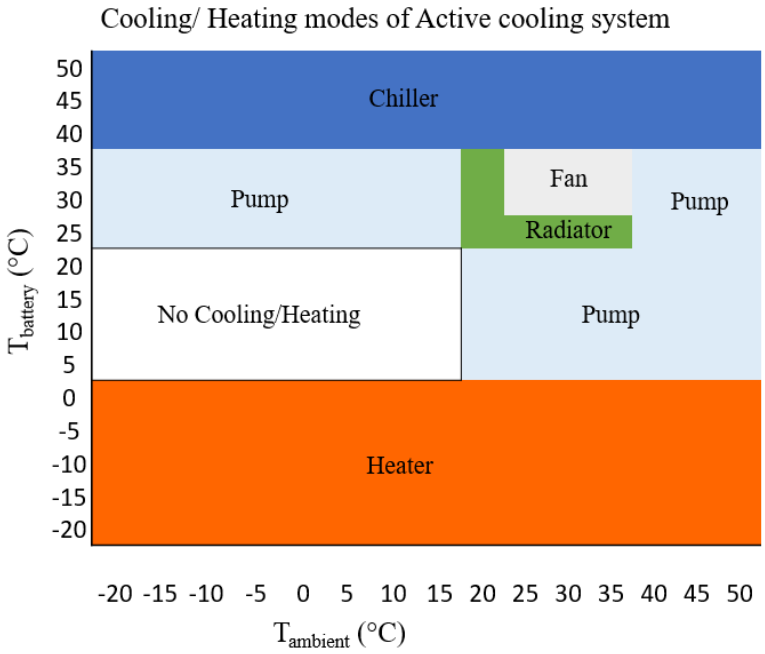

Figure 3.4: Thermal management strategy of actively cooled battery

The control strategy for switching of active components is represented in figure 3.4. The x, y-axes represent the ambient temperatures ($T_{ambient}$) and the battery temperatures ($T_{battery}$) respectively. It is varied between -20°C till 50°C, which is the recommended safe operating temperature range of this battery. The shaded regions represent the turning ON/ OFF of the various active components for the combination of $T_{ambient}$ and $T_{battery}$. For example, the chiller is turned ON, along with the fan and radiator when ambient temperature is atleast 20°C and the battery temperature increases above 35°C. Similarly, the heater is turned ON along with the action of the pump, when $T_{battery}$ decreases below 0°C and when $T_{ambient}$ increases above 20°C. The overall goal for the control strategy is to maintain the battery temperature within 0°C and 40°C for all load conditions.

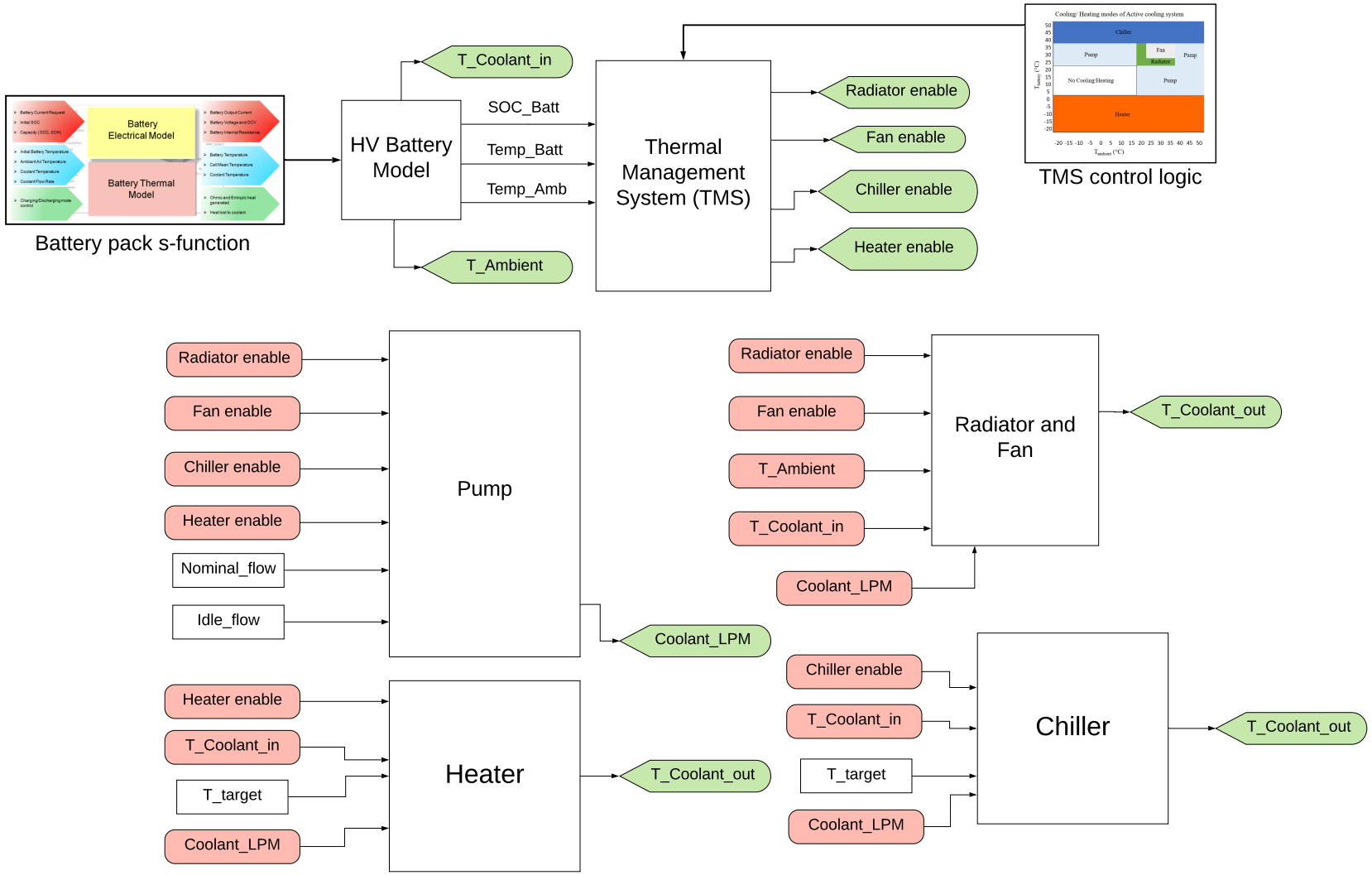

Figure 3.5: Thermal management system and active cooling components

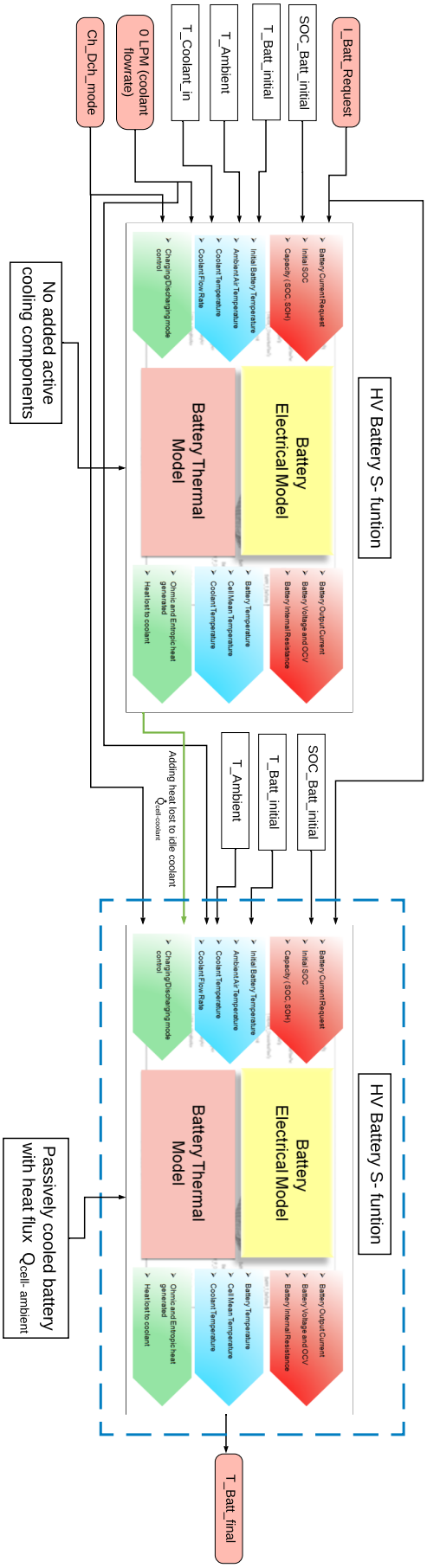

Figure 3.6: Passively cooled HV battery

3.3.2 Modelling of passive cooling system

The passive cooling system model is set up by using the battery s-function. The Simulink set up of the passive cooling system is shown in figure 3.6. The model uses two of the HV battery s-functions simultaneously, in order to compute the heat lost directly to the ambient atmosphere instead of the coolant.

$$\dot{Q}_{Res,Active} = \dot{Q}_{source} - \dot{Q}_{cells} - \dot{Q}_{TP} - \dot{Q}_{CP} - \dot{Q}_{coolant} \tag{3.1}$$

As described in section 2.5, the residual heat remaining in the battery responsible for temperature rise/drop, is the difference between the $\dot{Q}_{source}$ and $\dot{Q}_{sink}$. The heat sink, when using active cooling considers the thermal path shown in (3.1). The heat generated in the cells, flow through the thermal paste (TP), cooling plate (CP) and then finally into the coolant. The s-function is modelled containing this thermal path. The passive cooling could be modelled using a small work around using the s-function.

$$\begin{aligned} \dot{Q}_{Res,Passive} &= \dot{Q}_{source} - \dot{Q}_{cells} - \dot{Q}_{TP} - \dot{Q}_{CP} - \dot{Q}_{air} \\ \dot{Q}_{Res,Passive} &= (\dot{Q}_{Active} + \dot{Q}_{coolant}) - \dot{Q}_{air} \end{aligned} \tag{3.2}$$

The first HV battery s-function is used to calculate the heat lost to an idle coolant, $\dot{Q}_{coolant}$. Then this heat flux is added as input to the second battery s-function with the same configuration. Now, the second battery s-function is indirectly computing, $\dot{Q}_{Res,Passive}$ which is shown in (3.2). Now the complete model represented in fig. 3.6 indicating the heat transfer, $\dot{Q}_{cell-amb}$ taking place in a passively cooled HV battery instead of $\dot{Q}_{cell-coolant}$.

The convective heat transfer coefficient h, for this passive cooling simulation model is 10 $W/m2K$. In reality, h is directly proportional to the flowrate of air along the cooling plate surface, which is actually dependent on the vehicle speed. This relation is shown in Appendix A (fig. A.7). The value of h could be assumed as constant only for a forced passive cooling system like a fan, which would maintain constant air flowrate across the cooling surface.

3.4 Performance and Feasibility Analysis

An important objective of this project is to identify potential locations in the market which would be suitable for passively cooled HV batteries. Hence, a performance and feasibility analysis is required based on all its dependent conditions. Performance analysis techniques are popular amongst financial advisors, business analysts, supply chain managers and with many other professionals who have to forecast the results and make conclusions.

Typically, multivariate models are used to solve such problems. Analysts use these models, which has statistical tools that use multiple variables to forecast the possible outcomes. The Montecarlo simulation approach is widely used to create a probability distribution that gives a range of possible outcomes. The application of Montecarlo

simulations for performance analysis are discussed in [22]. A similar method of analysis, used in resilience engineering for an oil unit is discussed in [23]. The performance and feasibility analysis approach here is also multivariate but only deals with known outcomes. Hence, a simpler method called as weighted point evaluation algorithm is used.

3.4.1 Weighted Point Evaluation Algorithm

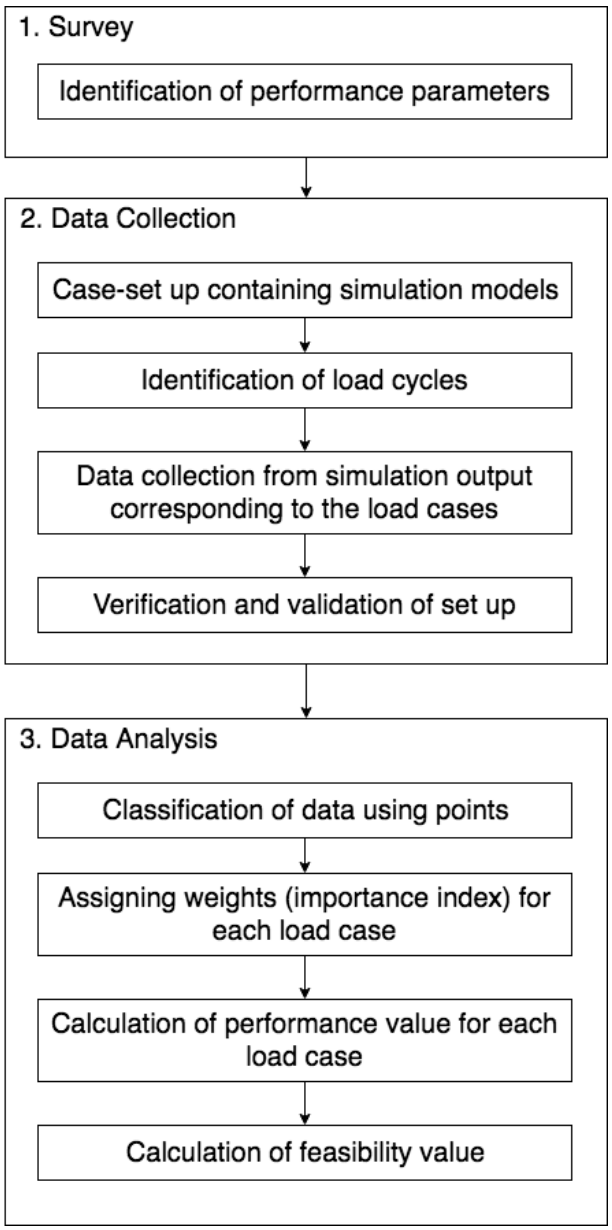

Figure 3.7: Flow chart of weighted point evaluation algorithm

The steps involved in a weighted point evaluation algorithm are shown in figure 3.7. Firstly, it begins with a literature survey and consolidation of performance parameters, which are the basis of our analysis. The performance parameters could be

represented as P_i, where $i = 1..., n$. The second step is data collection, which is done by n number of simulations or experiments. The number of different experiments is equal to the number of performance parameters. Then m, is the number of data generated per experiment or simulation. This data collected from the simulations or experiments have to be verified and validated, after which the complete data set available would be D_{ij}, where $i = 1, ...n$, $j = 1, ...m$.

In order to analyse the data, it has to be first segregated using points. Let f be the condition imposed to classify the data. Then, $f(D_{ij}) = p(k)$, where p is a point given to the data based on the classification condition. For example, the value of p could simply convey true or false, in that case p shall take the values either 1 or 0 and the value of k is 2. But, In certain cases we would like to classify the data based on comparative conditions like good, better, best, in which cases the value of $p(k) = 1, 2, 3$ and k here is 3. The number of classification cases k, could vary based on the imposed condition by the analyser.

After assigning points, the next step is to assign weights, also known as importance index. The weights have to be assigned for each simulation/ experimental condition. It is denoted as w_i and its value lies between 0 and 1. Hence, now the final values for the performance parameters is found by taking the product of the points and the corresponding weights that are assigned for it.

$$P_i = \sum_{i=1}^{N} \frac{p(k)w_i}{max(p)m} \tag{3.3}$$

The final numerical value calculated for performance parameters is given by P_i, as shown in (3.3). Further, the feasibility value has to be determined so that the analyst can compare different models using the simulations.

$$F(l) = (\sum_{i=1}^{N})P_i * 100 \tag{3.4}$$

The numerical value for feasibility of a system is obtained using (3.4). Here, l represents the number of systems chosen initially for the sake of comparison. The application of this algorithm is explained using an example later in the analysis chapter.

4

Results and Discussions

In this chapter we shall observe the results when the HV battery and cooling system models are simulated for various load cycles. The load cases chosen, are a combination of discharging and charging cycles introduced earlier in section 2.1.2. The simulation models discussed in the previous chapter, in the sections 3.2 and 3.3 are used to generate these results. Later in this chapter, tests are conducted to verify and validate the simulation set up, that is discussed.

4.1 Comparison of cooling system performance for different load cases

The results obtained in this section, require a common set of input conditions for the simulation model. These input values are presented in Table 4.1. The passively cooled and the actively cooled batteries are simulated separately for ambient temperature condition varying between -20°C to 50°C. Also, as discussed in the previous chapter, the main purpose of these simulations is to accumulate useful data. Then with MATLAB calculations, the performance and feasibility analysis of the two cooling systems are done, to identify a suitable choice for a market region

Table 4.1: Initial values for battery simulations

Ambient temperature(T_{amb})	-20...50°C
Battery initial temperature($T_{batt,initial}$)	equal to T_{amb}
Coolant temperature($T_{coolant,in}$)	$T_{batt,initial}$ + 2°C
SOC while charging	0 to 100%
SOC while discharging	100 to 0%
State of Health(SOH)	100%
Liquid cooling flowrate	0 to 6LPM

4.1.1 Rural discharge cycle performance

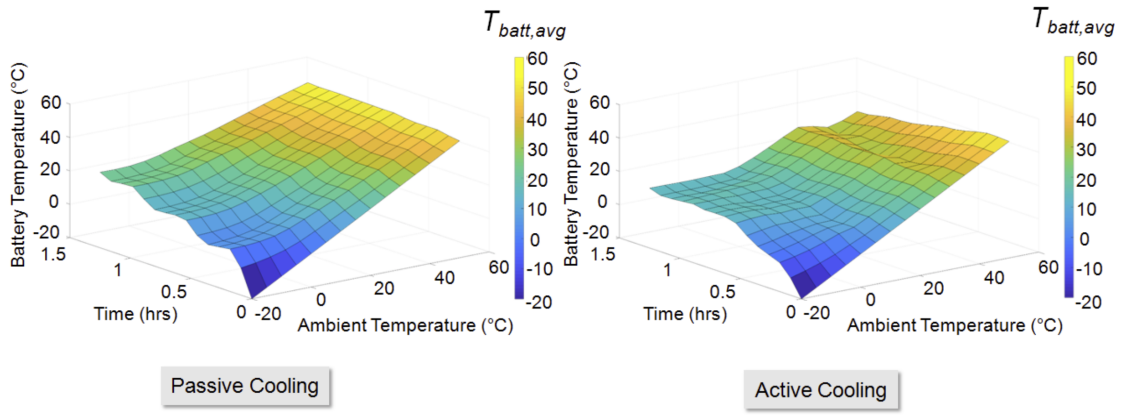

Figure 4.1: Average battery temperature for the Hakone drive cycle

A three dimensional representation of thermal states of the HV battery with passive or active cooling when subjected to the Hakone drive cycle is shown in figure 4.1. Here, the x-axis represents the ambient temperature (T_{amb}) condition which is also the battery initial temperature ($T_{batt,in}$). Then, the y-axis represents the discharging time taken for the battery to fall from 100% to 0% SOC and finally, the z- axis represents the battery average temperature ($T_{batt,avg}$) measured by the model at every time instant.

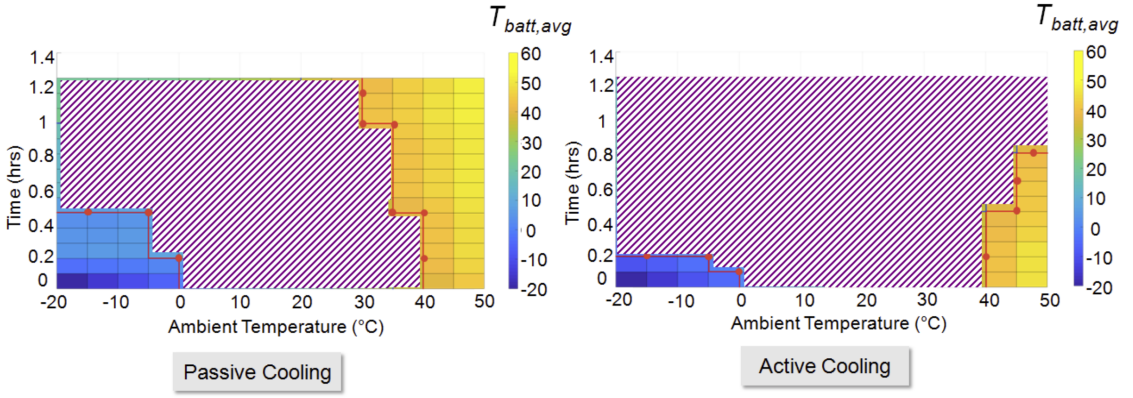

Figure 4.2: Projection of temperature profile for the Hakone drive cycle

A two dimensional graph obtained by projecting the same figure along z-axis is shown in fig. 4.2. The shaded region in purple represents those times during the discharge, when the average battery temperature is within 0°C and 40°C. This is the control temperature bandwidth set by the active cooling system strategy, hence it forms the basis for comparing the passively cooled counterpart.

Firstly, it is observed that the performance of passive cooling is as good as the active cooling for ambient temperatures between 0°C to 25°C. But, it seems to be limited

in the temperature regions either below or above it. For a temperature below 0°C, even though there is no heater available, the passively cooled battery is able to catch up, due to the irreversible, I^2R_{batt} heat generated. This is mainly due to the high internal resistance offered by the battery pack at low temperature and the aggressive discharge current from the Hakone drive cycle.

For ambient temperatures above 25°C, the passively cooled battery is heated beyond 40°C at the end of the rural discharge cycle. Due to the absence of a forced cooling mechanism like a chiller, it is not possible to control the passively cooled battery temperature below 40°C at the end of the Hakone drive cycle. It is only possible in an actively cooled battery. Hence, it is safe to say that a passively cooled battery is as good as an actively cooled battery for ambient temperature between 0 and 25°C for this load case.

4.1.2 Urban discharge cycle performance

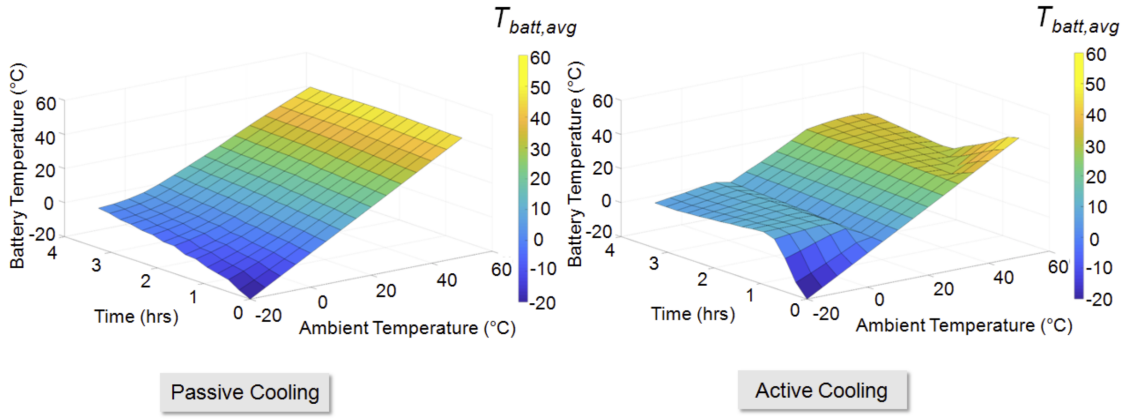

Figure 4.3: Average battery temperature for the JE05 drive cycle

The three dimensional thermal state of HV battery with passive or active cooling when subjected to JE05 drive cycle is shown in figure 4.3. The axes representation and initial conditions are the same as discussed earlier with rural drive cycle.

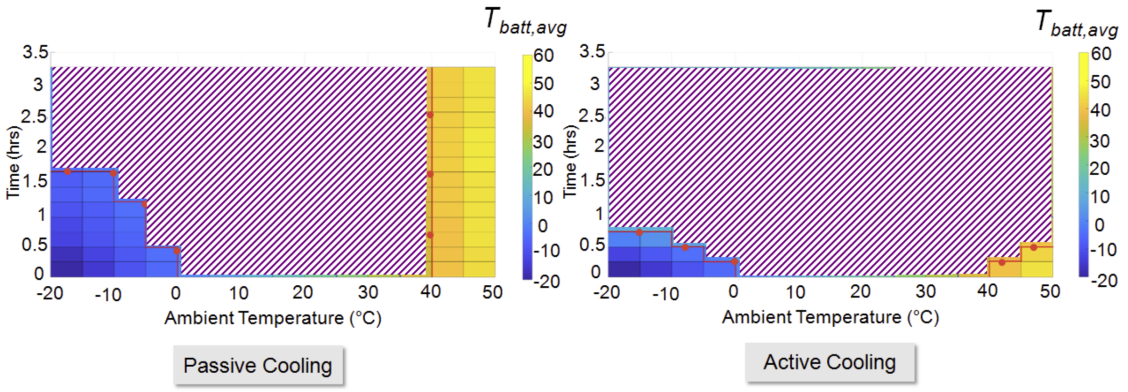

Figure 4.4: Projection of temperature profile for the JE05 drive cycle

Figure 4.4 is the two dimensional representation of the same graph with the shaded regions, showing the battery operation within 0°C and 40°C. The performance of an actively cooling system in maintaining the battery temperature within 0°C and 40°C has again worked well for this load case, especially in very low or very high ambient temperatures. Whereas, in the case of a passively cooled batteries, it requires a long time, (i.e) it would take at least an hour for the battery to heat up above 0°, when the ambient temperature is below -5°. Also, it is not possible to cool down a passively cooled battery to stay within the control temperature limit for the ambient temperatures beyond 40°C.

Hence, it is safe to say that a passively cooled battery is as good as an actively cooled battery for ambient temperatures between 0°C and 40°C for the urban load case.

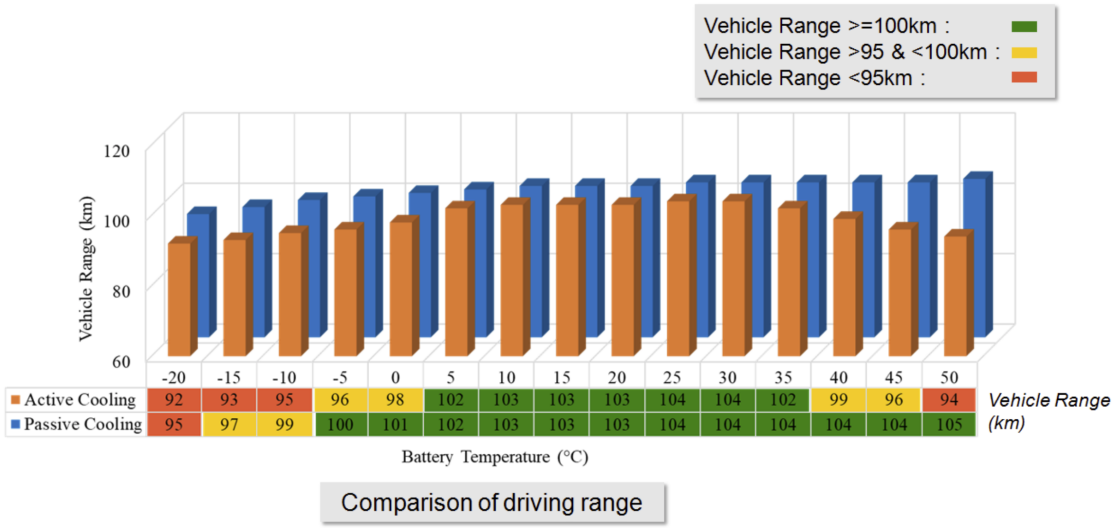

	-20	-15	-10	-5	0	5	10	15	20	25	30	35	40	45	50
Active Cooling	92	93	95	96	98	102	103	103	103	104	104	102	99	96	94
Passive Cooling	95	97	99	100	101	102	103	103	103	104	104	104	104	104	105

Vehicle Range (km)

Figure 4.5: Comparison of driving range offered for the JE05 drive cycle

The comparison of driving range offered by the passively and actively cooled electric vehicles is shown in figure 4.5. This range is computed for the vehicle for the

standard JE05 drive cycle. It is clearly seen that, the passively cooled batteries are capable of providing an average 5 km more driving than the actively cooled batteries. This is because in a passively cooled battery, weight is reduced due to the absence of active cooling components. The available energy for driving is more since the added components consume energy directly from the HV battery for their operation. The range values are marked with colors green, yellow and red corresponding to the limits mentioned in the legend. This segregation is required while calculating the performance and feasibility values using the weighted point evaluation.

Interestingly, there are some range losses even with the case of the LDT with passively cooled batteries. The vehicle range offered by passively cooled LDT are less than 100 km for ambient temperatures less than -5°C, because the battery internal resistance offered in these conditions are significantly high and hence lead to ohmic losses in the passively cooled batteries.

4.1.3 Quick charge cycle performance

DC quick charging is another important performance parameter for electric vehicles. The key concerns during the 50 kW DC charging event, are the battery operational temperature and the time taken to reach full charge (from 0% to 100% SOC). The initial conditions required in the simulation model is the same as discussed earlier.

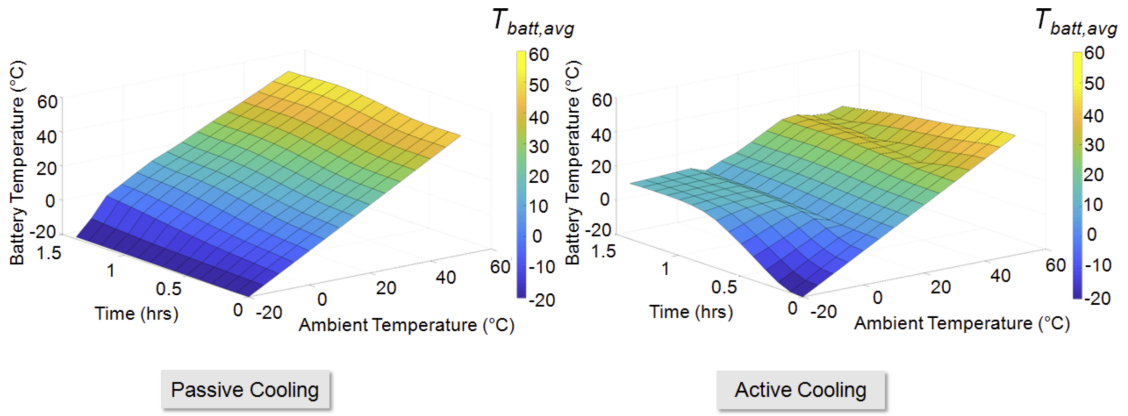

Figure 4.6: Average battery temperature during the 50 kW DC charging event

Figure 4.6 shows the battery temperature profile for a DC charging event conducted for 1.5 hrs. The simulation time of 1.5 hrs is chosen based on customer demand to fast charge the vehicle.

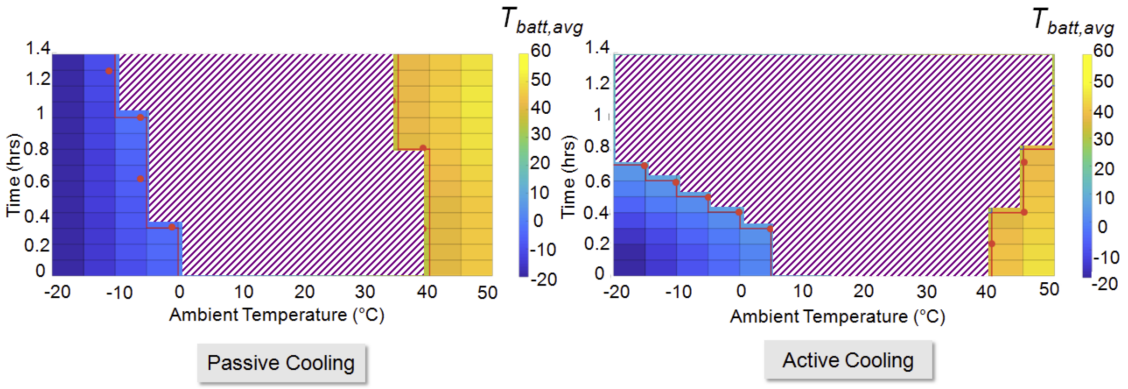

Figure 4.7: Projection of temperature profile for 50 kW DC charging

The 2D representation of the battery temperature profile is shown in figure 4.7. The shaded region compares passively and actively cooled battery operation between temperature 0°C and 40°C. Similar to the urban discharging load cycle, the DC charging load cycle is not capable of heating the passively cooled battery above 0°C when the ambient temperature is below -5°C. This is mainly due to limitation of maximum charging current to avoid Li plating (as shown in fig. 2.9) and insufficient production of I^2R_{batt} heat for battery temperatures below 0°C.

When the ambient temperature is 35°C and above, the passively cooled battery heats beyond 40°C. Without active cooling components, it is not possible to increase or decrease the battery temperature to stay within the required control limits. Hence, it is safe to say that a passively cooled battery is as good as an actively cooled battery for the ambient temperatures between 0°C and 35°C for the 50 kW DC charging load case.

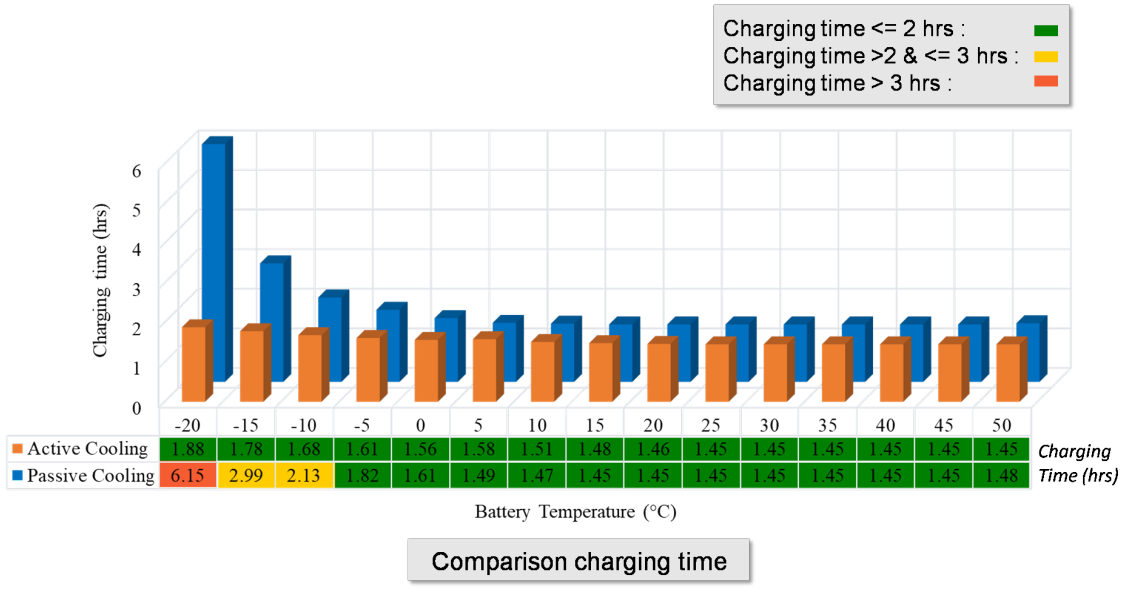

Figure 4.8: Comparison of charging time for 50kW DC charging

The next important aspect to be studied is the charging time, typically electric vehicles are required to be DC charged from 0% to 100% SOC within 2 hrs. The comparison of DC charging time for the electric truck with passive and active cooling systems are shown in figure 4.8.

The ambient temperature for which the charging time is within 2 hrs are marked with green, with charging time lying between 2- 3 hrs are marked with yellow and when it takes longer than 3 hrs, it is marked with red. A passively cooled battery takes longer charging time than actively cooled battery for temperatures below -5°C. For the ambient temperature -20°C, it can take as much as 6.15 hrs to charge which defeats the purpose of quick charging. It is again, mainly because of the fact that the maximum charging current is highly limited by the BMS to protect against Li-plating during the low battery temperatures. Since, there is no heater available in the passive system to increase the battery temperature above 0°C, it is only possible to charge with the limited battery current. The charging load is only used to self-increase the battery temperature above 0°C, beyond which there are no limitations on the maximum charging current.

For ambient temperatures above 0°C, the charging time taken for the passively cooled and the actively cooled batteries are the same.

4.1.4 Maximum load cycle performance

So far, the battery performance for either the charging or the discharging events were studied individually. But practically, it has to be studied as a combination. From the considered load cycles, a hakone rural discharge cycle followed by 50 kW DC quick charging event would provide the maximum electrical load condition on the HV battery.

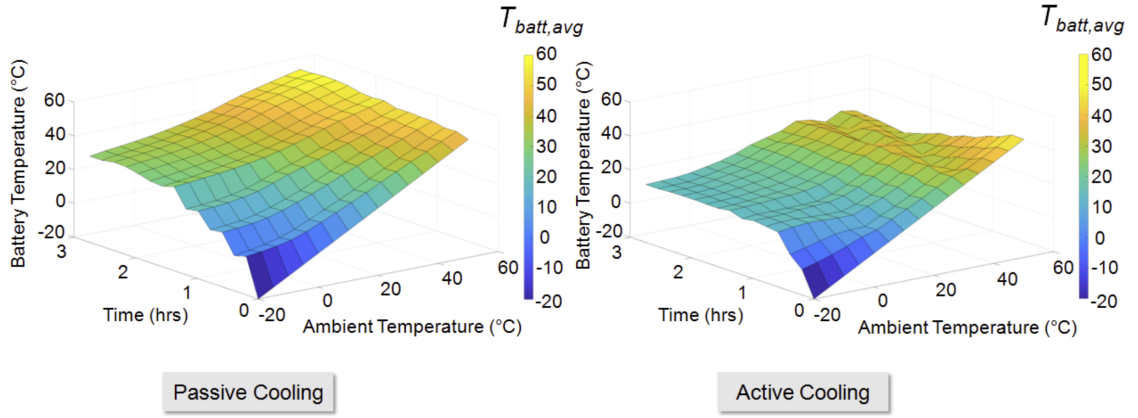

Figure 4.9: Average battery temperature for the maximum load cycle

The battery is discharged using the hakone drive cycle from 100% SOC to 0% and then charged back to 100% using the DC quick charging cycle. Figure 4.9 shows the temperature profile for this maximum load cycle.

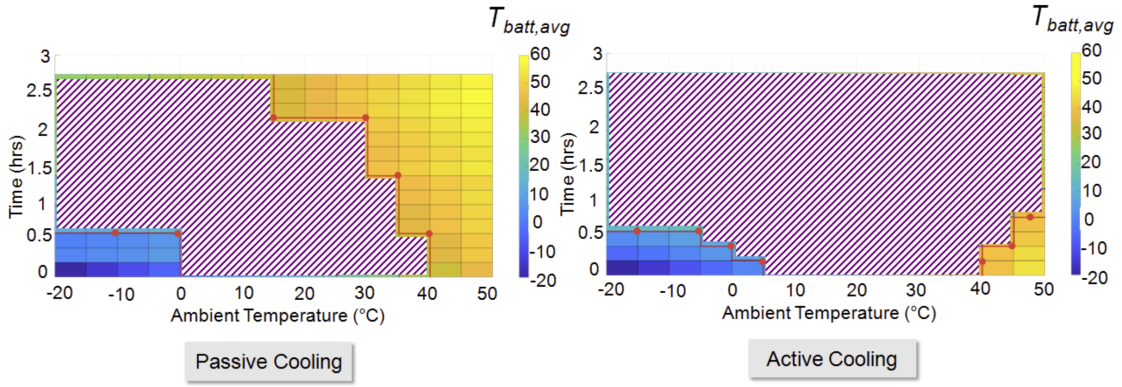

Figure 4.10: Projection of the temperature profile of the maximum load cycle

The 2D projection of the temperature profile is shown in figure 4.10. It clearly shows that for the ambient temperatures between -20°C and 15°C, the passive cooled battery is operated within the active cooled battery's control temperature limit.

But beyond the ambient temperature of 15°C, the passive cooled battery heats beyond the controlled limit due to the maximum load. The cooling offered by the passive system is insufficient and hence, an actively cooled battery is recommended for these ambient temperature conditions.

4.1.5 Nominal load cycle performance

As the name suggests, a nominal load cycle is the combination of discharging and charging events that the battery undergoes usually in an electric light duty truck (LDT).

For this simulation, the battery would be discharged from 100% to 0% SOC using the JE05 drive cycle and then it would be chaged back to 100% SOC using the 50 kW DC charging event. This load cycle is considered since, majority of this electric LDT's customers use these as convenient store or supermarket delivery vehicles. They are continuously functioning on quick charging and driving in the city but, they are not as demanding as the maximum load cycle.

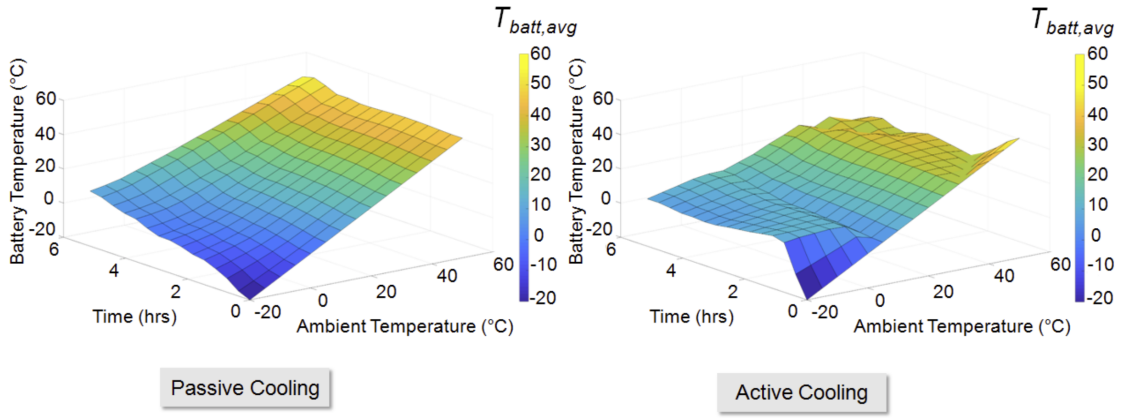

Figure 4.11: Average battery temperature for JE05 discharge followed by DC charging

The battery is discharged using the JE05 urban drive cycle from 100% to 0% SOC and then, it is charged backed to 100% SOC using the DC quick charging cycle. The battery thermal state for the nominal load cycle is shown in figure 4.11.

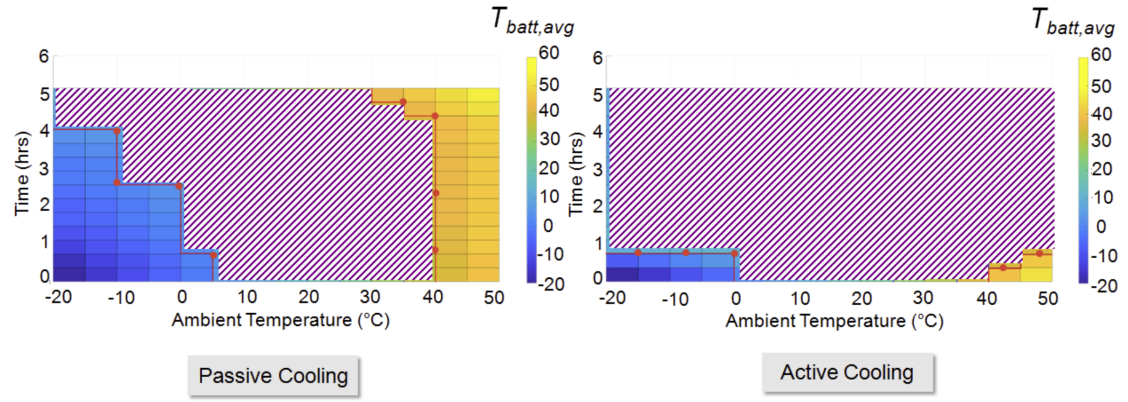

Figure 4.12: Projection of temperature profile for nominal load cycle

The 2D projection of the battery temperature profile is shown in figure 4.12. It clearly shows that for the ambient temperatures between -20°C to 30°C, the passively cooled battery is operated within the actively cooled battery's control temperature limit. But for the ambient temperatures, higher than 35°C, the passively cooled battery's temperature increases beyond 40°C. The cooling offered by the passive system is insufficient and hence, actively cooled battery is recommended for these ambient temperature conditions.

Similarly, for the ambient temperatures below -10°C, the passive cooled battery finally reaches above 0°C only at the end of the nominal load cycle. However, for faster heating up of battery during low ambient temperatures, an active cooling system is highly recommended.

4.2 Verification and Validation of Simulation

4.2.1 Validation of HV battery and active cooling simulation with test vehicle

Since the performance and feasibility of the passively cooled battery is done against the actively cooled counterpart, it is important to validate the base simulation model. The HV battery s-function behavior with an active cooling system model in MATLAB is validated by comparing it with the actual vehicle's battery system. In order to obtain a constant current load to the HV battery, the electric truck must be driven on a flat surface at a constant speed, with almost zero acceleration.

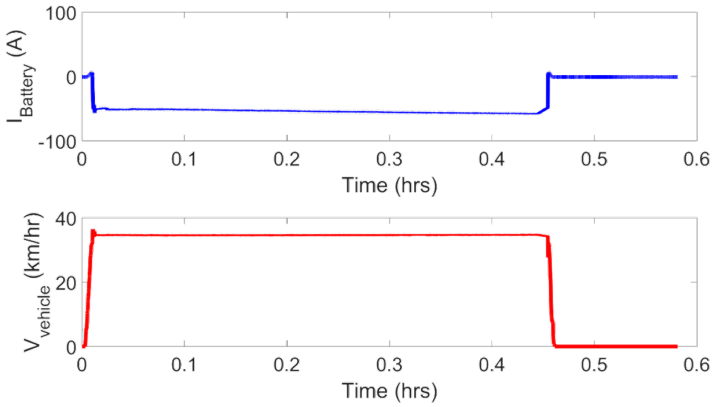

Figure 4.13: Constant load to HV battery in a test vehicle setup

The test truck operates at constant velocity of 35 *kmp* on a flat test bed, the vehicle velocity and the current request profiles recorded are shown in the figure 4.13. After a time span of 30 mins, the test truck is brought to stop.

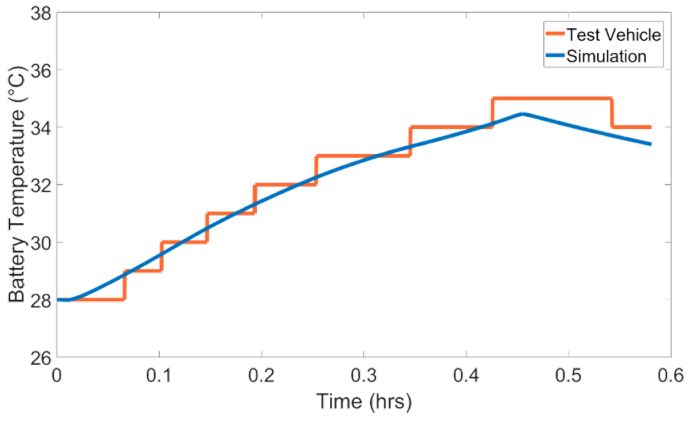

Figure 4.14: Comparison of test vehicle's battery and simulation battery temperature

The temperature profile of the test vehicle's HV battery for this constant load condition is shown in figure 4.14. The same test is simulated in MATLAB for the HV

battery with active cooling system. The ambient temperature (T_{amb})is 25°C, initial battery temperature ($T_{batt,in}$) is 28°C and coolant inlet temperature ($T_{coolant,in}$) is 27°C. The coolant flow in the active cooling system is 6 LPM. The temperature profiles from simulation and the actual vehicle coincide well, which means that the MATLAB simulation of the HV battery with an active cooling system corresponds well with the real scenario. The battery temperature gradually rises from 28°C to 35°C and then due to the functioning of the chiller and the removal of load to the battery, the temperature begins to drop. This test validates the active cooling simulation model, which is the base system for comparison in this thesis.

4.2.2 Comparison of cool down performance between passive and active

The constant load test provides an idea of heat accumulation in the battery. Consequently, it is also quite interesting to study and compare the heat rejection from the battery, when using the two cooling systems.

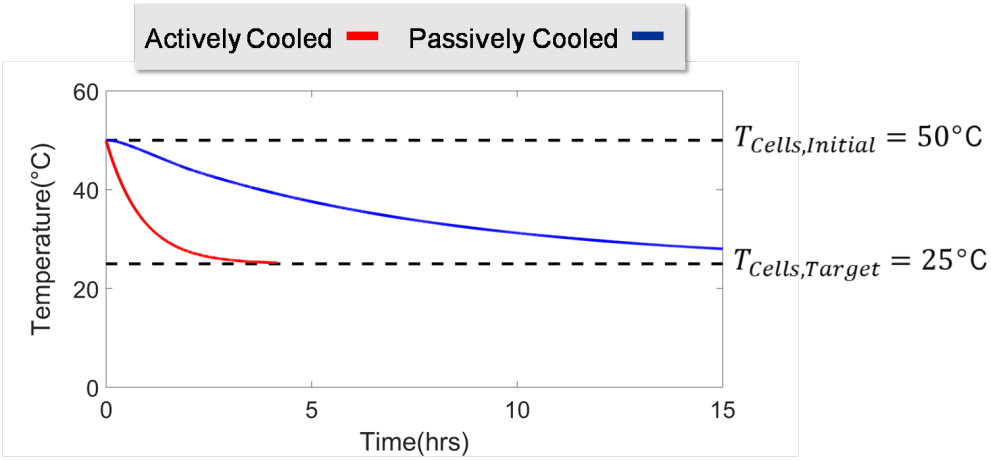

Figure 4.15: Comparison of cooling performance

Figure 4.15 shows the cooldown curves for the HV battery from 50°C to 25°C. The initial conditions for the simulation are as follows, $T_{batt,in}$= 50°C, T_{amb}= 25°C, $T_{coolant,in}$= 27°C and the coolant flowrate is equal to 6 LPM. The falling battery temperature profile is similar to first order electrical RC circuit's fall in voltage for constant discharge current. The thermal equivalent RC representation and the relation representing instantaneous T_{batt}, as a function of $\dot{Q}$, R_{th} and C_{th} is given in section (2.5).

Table 4.2: Calculated parameters of the cooling systems

Parameters	Actively cooled	Passively cooled
Total cooling time (hrs)	3.45	>15
Time constant $\tau(hrs)$	0.86	7.2
R_{th} (K/kW)	26	233
C_{th} (J/K)	112,000	112,000
$\dot{Q}$ (kW)	0.899	0.108

Table 4.2 presents the physical values corresponding the cool down curve shown in fig. 4.15. The thermal resistance, R_{th} and capacitance, C_{th} values corresponding to the two types of battery packs are explained briefly in Appendix A (section A.1.2). The time constant of the profile (τ) is the time taken to reach 63% of final battery temperature which is 34.25°C. Hence the values presented as τ for actively and passively cooled is the time taken for the battery to fall from 50°C till 34.25°C.

$$\tau = R_{th}C_{th} \tag{4.1}$$

The relationship between thermal parameters and time constant, τ is given by (4.1).

$$\dot{Q} = \Delta T/R_{th} \tag{4.2}$$

Subsequently, the value of the heat flux, is calculated using (4.2). On comparing the $\dot{Q}$ values obtained for the active and passive cooling system, it is observed that the heat rejection rate using active cooling is 10 times faster than using passive cooling. These numerical figures are important while comparing overall performance of the two cooling systems.

5

Performance and Feasibility Analysis of Cooling system models

5.1 Overall performance of the cooling system for different ambient temperature conditions

5.1.1 Cumulative temperature data for all loads

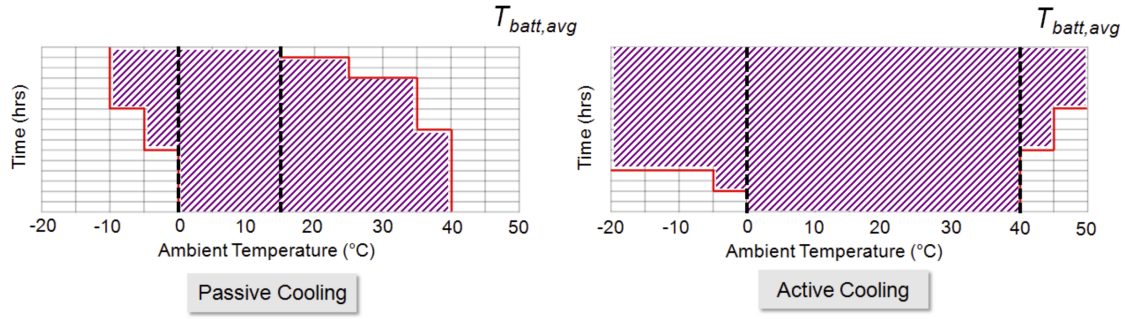

Figure 5.1: Projection of cumulative battery temperature profiles

The cumulative battery temperatures for the five load cases (rural, urban, maximum, nominal and DC charging), lying within the range 0°C and 40°C are shown in fig. 5.1. It is the sum of all the shaded regions represented in the 2D projections of the battery temperature profiles. The x-axis represents the ambient temperature of varied from -20 to 50°C and the y-axis represents the simulation time. The simulation time corresponds to the charging or discharging time taken for the HV battery, its values set shall differ based on the nature of the chosen load case.

The comparison shows that for the ambient temperatures between, 0°C and 15°C, a vehicle with a passively cooled battery is as good as a vehicle with an actively cooled battery. This is because, the battery operation temperature in this region lies within the control temperature range for all the considered load conditions. This makes the passively cooled battery suitable for the electric trucks sold in the market regions with ambient temperatures varying between 0°C and 15°C.

5.1.2 Cumulative temperature data excluding rural load condition

Since, these electric LDTs are practically used as delivery vehicles for convenience stores, the rural load cycle could be neglected, in order to obtain a realistic feasibility from the analysis.

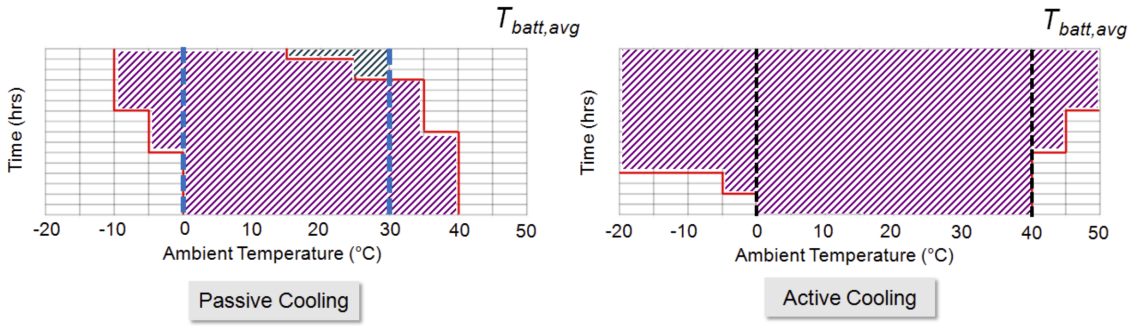

Figure 5.2: Projection of cumulative battery temperature profiles except rural discharging loads

The cumulative battery temperatures lying, within the range 0°C and 40°C is shown in fig. 5.2 considering the load cases, excluding the mountainous rural cycle. The comparison shows that for ambient temperature conditions lying between 0°C and 30°C, a vehicle with passive cooled battery is as good as a vehicle with an actively cooled battery. The passively cooled battery operation temperatures lies within the expected control temperature range. There is an extension in the possible markets for the passively cooled batteries when compared to the previous case since, the rural load cycle has now been removed from the performance and feasibility analysis.

5.1.3 A curious case study of Tokyo

Tokyo is the most eligible consideration as a market location for this electric light duty truck due to its populous metropolitan nature and huge demand for delivery vehicles from its convenience stores. This section investigates the performance and feasibility of passively cooled HV batteries against its actively cooled counterpart using the algorithm mentioned in 3.4.1. The main inputs to begin with are average temperature distribution and customer load cycles.

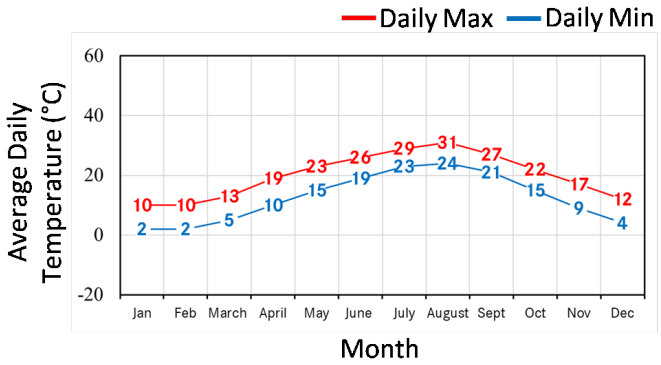

Figure 5.3: Average monthly temperature distribution in Tokyo, Japan

The monthly average ambient temperature distribution of Tokyo is shown in figure 5.3. The algorithm begins with identification of performance parameters. Considering the two main inputs for the cooling system, the common parameters for comparison are chosen to be the battery temperature for discharging, charging, maximum and nominal load conditions, the range offered by the vehicle for an urban drive cycle and then, the DC charging time.

Data is collected using the battery simulation set up in Simulink, for all the mentioned load cases with the ambient temperatures being varied from -20°C to 50°C. Then, the average daily temperature of market location, Tokyo, is found by taking the average of its maximum and minimum monthly temperature value. This is the initial state for the analysis (weighted- point) algorithm in MATLAB. For these monthly (twelve) temperature values, The final state data like operation temperature, vehicle range and charging time are found out. The final state data (T_{batt}, vehicle range, charging time) obtained for the chosen market location is segregated based on the conditions shown in Table 5.1.

Table 5.1: Points table to analyse simulation data

Final state data (D)	Condition ($f(D)$)	Point assigned (p)
Temperature (T_{batt})	25 to 35°C	3
	0 to 40°C	2
	<0 and >40°C	1
Vehicle Range	>100km	3
	>95 to <100km	2
	<95km	1
Charging Time	<= 2hrs	3
	>2 to <= 3hrs	2
	>3hrs	1

The points assigned to the segregated data are 3,2,1 with the value of importance decreasing from 3 to 1. The next step is to provide weight-age to the segregated data and compute the performance parameters and feasibility values. The importance index or the weights are assigned to the segregated data as shown in the Table 5.2.

Table 5.2: Points table to analyse simulation data

Final state data (D)	Load cycle	Weights (w)
Temperature (T_{batt})	Rural cycle	0.12
	Urban cycle	0.12
	50kW DC charge	0.12
	Maximum load	0.17
	Nominal load	0.17
Vehicle Range	Urban cycle	0.15
Charging Time	50kW DC charge	0.15

The weights take values between 0 to 1 according to their impact in the overall performance. Since, the objective of this analysis is the comparison and evaluation of two cooling systems, the battery temperature data carries more importance than the vehicle range delivered or the charging time. Within the temperature data, Only charge or discharge load cycle data is assigned less weight-age than a combined load cycle(maximum or nominal), since they are more likely to occur in the practical scenario.

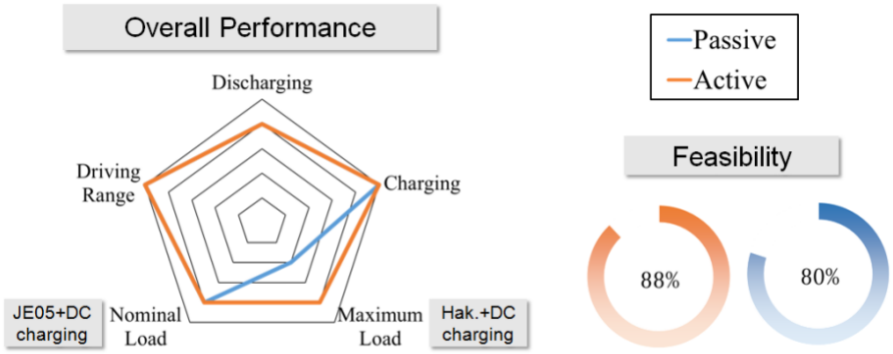

Figure 5.4: Performance and feasibility of passively cooled batteries for Tokyo

Finally, next step is to calculate values of performance parameters P and feasibility F, defined in (3.3) and (3.4). In this analysis, the value of number of states N= 7, number of simulations equal to number of ambient temperature conditions, which is m= 12. Using these values separate performance values are found out as a fraction of 5 and represented in the spider diagram shown in figure 5.4. Then, finding the cumulative sum of performance percentage using (3.4), The feasibility of the cooling system for the market location is presented out of 100% in the same figure. Similar results calculated for Phoenix (Arizona), a hot market region and Kiruna, a cold market region are presented in the Appendix B.

The inference from the analysis report shows that passive cooling works as good as active cooling for the HV battery in Tokyo. The passive cooled battery can not be recommended for a vehicle in Tokyo which shall have an heavy discharging load cycle, because passive cooling can not control the rise in battery temperature. Oper-

ating the battery in uncontrolled high temperatures will also accelerate the ageing of cells. Hence, there is a decrease in performance for such loads, which is represented in the maximum load performance parameter.

However, by excluding the customer sales that require heavy discharging loads in Tokyo, the feasibility values passively cooled and actively cooled batteries are almost the same, which are 80% and 88% respectively. This means that passively cooled batteries could definitely be considered for the future LDTs sold in Tokyo, Japan. Interesting performance and feasibility results for market regions, Phoenix, Arizona in the USA and Kirun, Sweden are presented in figures B.1 and B.2.

5.1.4 Cost Analysis

The final task involved to complete this performance and feasibility check of passively cooled batteries for electric LDT's is its cost analysis. The cost of a Li-ion battery used for EV application as discussed in [24] is about 275£/kWh. When calculated for the HV battery used in this LDT, the cost is 22,500£ as shown in table5.3. The cost of the active cooling system components consisting of radiator and fan, chiller, heater, pump, pipes and coolant reservoir are also estimated in the same table.

Table 5.3: Cost of a HV battery and its cooling system components

Component	Price(£)
HV Battery	22500
Radiator and fan	240
Chiller	75
heater	200
Pump	100
Pipes	1800
Coolant reservoir	65

The cost of passively cooled battery is just equal to net estimated cost of the HV battery. But the cost of an actively cooled battery is the sum of cost of battery along with the cost of all the active components.

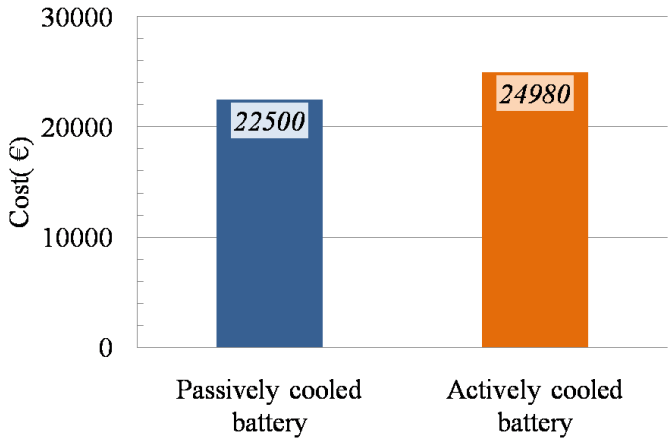

Figure 5.5: Cost comparison of passively and actively cooled battery

The total cost of the passively cooled and actively cooled batteries are shown in the figure 5.5. The active cooling components sum up to 2,500£ separately. By adopting a passively cooled battery in electric trucks, there would be a net saving of 11% of the battery's cost due to the absence of these active components.

6
Conclusion

The various analysis and results obtained in this thesis now suggests that, passively cooled batteries in the electric LDT's are feasible for the market regions lying within the ambient temperature range, 0 to 15°C. Further, the saleable market regions could be increased for a wider ambient temperature range, by the exclusion of the higher power demanding, rural drive cycle from the analysis. Now, the trucks could also be sold in the markets regions lying within the ambient temperature range, 0 to 30°C.

Even though the rate of cooling was found to be 10 times slower in passively cooled batteries, it still full fills all the performance criterion expected by the LDT customers based on safe battery operating temperatures, driving range and DC fast charging time.

Furthermore, moving towards passively cooled batteries in the recommend regions would lead to a 11% saving in the battery development cost, reduce the number of added components and would provide an extra 5 km driving range.

6.1 Future work

As much as the average battery temperature which is used for analysis in thesis, it equally important to study the individual cell temperature spread, ΔT_{cell} across the battery pack. This would indicate the thermal imbalance in the pack and would also allow the engineer to address the problems like cell ageing. Hence, improving the simulation set up including the determination of ΔT_{cell} across the cells is an interesting work for future from this thesis.

Also, the passive cooling model set up in this simulation does not account for the unequal cooling across the pack, but rather considers a constant and equal heat transfer throughout. This is not true in the real case and heat transfer co-efficient has to be obtained in different locations of the pack as a function of the vehicle or the external wind speed.

Since, this setup forecast battery temperature for different loads and ambient temperature. The next step would be to develop an online estimation setup in the vehicle which could predict the change in battery temperature in the forthcoming instants. This would also help to efficiently use the active cooling strategy in combination with passive and other modes of cooling, leading to energy saving.

Representation of new types of cooling systems from literature and researches as simply combination of R_{th} and C_{th}, would help to standardize, compare and analyse all types of cooling/ heating methods which might be developed in future.

6.2 Sustainability and Ethics

Li-ion battery driven commercial electric vehicles are undoubtedly a great initiative towards sustainable transportation because, it puts an end to the usage of fossil fuels and its associated emissions. However, this promotion has been going on for almost a decade now and has led to other secondary concerns like reducing and recycling Li-ion batteries.

The demand for battery cells have led to abusive mining of Lithium (Li) and Cobalt (Co), violating human rights in places Argentina and Congo. Hence, the Amnesty International has agreed to give equal importance to watch human rights as much as it would support to solve the climate crisis. This constantly drives researches and scientists to come up with commercially viable battery cell replacements.

Passively cooled batteries in electric vehicles are considered as a sustainable solution because, it could be adapted to all newly developed battery cell technologies. It advocates lean battery development with minimum components which would largely improve the sustainability data shown in its supply chain. The OEMs should sell passively cooled vehicles responsibly to their customers when they claim competitive performance values because it largely depends upon the market's ambient and usage conditions.

Bibliography

[1] Zhonghao Rao, Shuangfeng Wang, 'A review of power battery thermal energy management', China. Available online: 15 September 2011.

[2] Ahmad A. Pesaran, Ph.D., Andreas Vlahinos, Ph.D., Steven D. Burch, ' Thermal Performance of EV and HEV Battery Modules and Packs', Fourteenth International Electric Vehicle Symposium Orlando, Florida, December 1997.

[3] C. Huber, R. Kuhn, 'Thermal management of batteries for electric vehicles', Singapore.

[4] Ahmad A. Pesaran, ' Battery Thermal Management in EVs and HEVs: Issues and Solutions, Advanced Automotive Battery Conference, Las Vegas, Nevada, February 2001.

[5] A.A Pesaran, S. Burch and M. Keyser,' An Approach for Designing Thermal Management Systems for Electric and Hybrid Vehicle Battery Packs', National Renewable Energy Laboratory, May 1999.

[6] Lars Ole Valøen, Mark I. Shoesmith, 'The Effect of PHEV and HEV Duty cycles on Battery and Battery Pack Performance', available on: http://umanitoba.ca/outreach/conferences/phev2007/PHEV2007/proceedings/PluginHwy_PHEV2007_PaperReviewed_Valoen.pdf

[7] Jiling Li, Zhen Zhu, ' Battery Thermal Management Systems of Electric Vehicles', Master Thesis in Automotive Engineering, Chalmers University of Technology, Sweden 2014.

[8] Shuai Ma, Modi Jiang, Peng Tao, Chengyi Song, Jianbo Wu, Jun Wang, Tao Deng, Wen Shang, 'Temperature effect and thermal impact in lithium-ion batteries: A review', Progress in Natural Science : Materials International, November 2018.

[9] Yu Miao, Patrick Hynan, Annette von Jouanne and Alexandre Yokochi, 'Current Li-Ion Battery Technologies in Electric Vehicles and Opportunities for Advancements', energies, March 2019.

[10] Article BU-205 : 'Types of Lithum-ion', available online : https://batteryuniversity.com/learn/article/types_of_lithium_ion

[11] 'ACEA Tax guide', 2018, European Automobile Manufacturers Association, Available on: https://www.acea.be/uploads/news_documents/ACEA_Tax_Guide_2018.pdf

[12] Maximilian Holland, Dr., '2019 Nissan LEAF — Still No Liquid-Cooled Battery?', December 2018,
Available on: https://cleantechnica.com/2018/12/05/60-kwh-nissan-leaf-still-no-liquid-cooled-battery/

[13] Jack Stewart, 'The Neat Engineering VW Used to Smash the Pikes Peak Record', June 2018, Available on: https://www.wired.com/story/engineering-ofthevwpikespeakbattery/

[14] Heesung Park, 'A design of air flow configuration for cooling lithium ion battery in hybrid electric vehicles', Journal of Power Sources, March 2013.

[15] 'Cooling Electric Vehicles', Dober,
Available on: https://www.dober.com/electric-vehicle-cooling-systemselectric_vehicle_thermal_management_system

[16] Cristophe Forgez, Dinh Vinh Do, Guy Friedrich, Mathieu Morcrette, Charlers Delacourt, ' Thermal Modeling of a cylindrical $LiFePO_4$/ graphite lithium-ion battery, Journal of Power Sources, November 2009.

[17] Xinfan Li, Hector E. Perez, Shankar Mohan, Jason B. Siegel, Anna G. Stefanopoulou, Yi Ding, Matthew P. Castanier, 'A lumped-parameter electro-thermal model for cylindrical batteries', Journal of Power Sources, January 2014.

[18] Yonghuang Ye, Yixiang Shi, Lip Huat Saw, Andrew A.O Tay, 'Performance assessment and optimization of a heat pipe thermal management system for fast charging lithium ion battery packs', International Journal of Heat and Mass Transfer, September 2015.

[19] Ki-Yong Oh, Bodgan I. Epureanu, 'A phenomenological force model of Li-ion battery packs for enhanced performance and health management', Journal of Power Sources, August 2017.

[20] Yuanwang Den, Changling Fengm Jiaqiang E, Hao Zhu, Jingwei Chen, Ming Wen, Huichun Yin, 'Effects of different coolants and cooling strategies on the cooling performance of the power lithium ion battery system: A review, Applied Thermal Engineering, October 2018.

[21] 'Heat transfer applications using 3M Novec Engineered Fluids', November 2018, available on: https://multimedia.3m.com/mws/media/1091997O/3m-novec-engineered-fluids-for-heat-transfer-line-card.pdf.

[22] Gabor Belvardi, Andras Kiraly, Tamas Varga, Zoltan Gyozsan, Janos Abonyi, 'Monte Carlo simulation based performance analysis of supply chains', International Journal of Managing Value and Supply Chains (IJMVSC), January 2012.

[23] Masoud Rabbani, Reza Yazdanparast, Mahdi Mobini, 'An algorithm for performance evaluation of resilience engineering culture based on graph theory and matrix approach', Published online : 21 February 2019.

[24] Article BU-1003 : 'Electric Vehicle(EV)', available online : https://batteryuniversity.com/learn/article/electric_vehicle_ev

[25] John Warner, 'Handbook of Lithium-Ion Battery Pack Design - Chemistry, Components, Types and Terminology', Elsevier, 2015.

[26] Victor Strängberg,'Cell characterization and modeling of lithium ion batteries', Bachelor Thesis in Electric Power Engineering, Chalmers University of Technology, Sweden 2016.

[27] Avnish Narula, 'Modeling of Ageing of Lithium- Ion Battery at Low Temperatures', Master of Science Thesis in Electric Power Engineering, Sweden 2014.

[28] Anton Lidbeck, Kazim Raza Syed,'Experimental Characterization of Li-ion Battery cells for Thermal Management in Heavy Duty Hybrid Applications', Master of Science Thesis in Electric Power Engineering, Sweden 2017.

[29] Aleksandra Baczynska, Waldemar Niewiadomski, Ana Gonçalves, Paulo Almeida and Ricardo Luís, 'Li-NMC Batteries Model Evaluation with Experimental Data for Electric Vehicle Application', Published online : batteries, MDPI, February 2018.

A

Appendix 1

A.1 Simplified Electro-Thermal Modelling of HV Battery

A.1.1 Electrical equivalent circuit

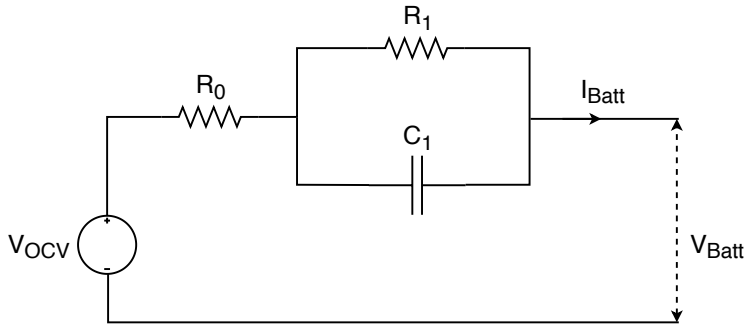

Figure A.1: RC equivalent circuit of Li-ion battery

With the known values of battery open circuit voltage (V_{OCV}) and RC values of the electrical equivalent circuit shown in figure A.1, one could determine the battery current, I_{Batt} and voltage, V_{Batt}.

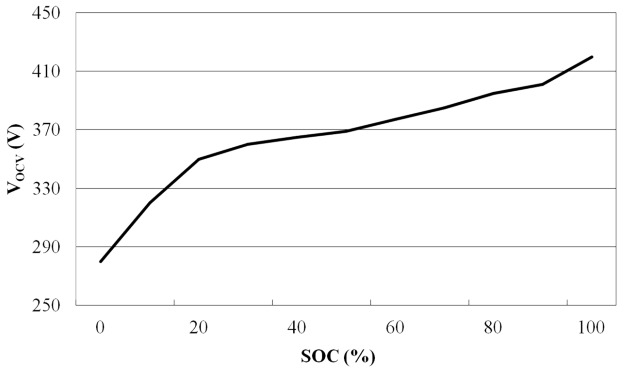

Figure A.2: OCV of battery as a function of SOC

Figure A.2 shows the variation of battery OCV as a function of its state of charge (SOC). The profile belongs to a HV battery pack containing 100 NMC Li-ion cells

in series.

The resistance R_0 in the equivalent circuit represents the ohmic resistance of the battery and the impedance from the parallel combination of R_1, C_1 offer the effect of charge transfer and mass transport in the cells. Table A.1 shows the equivalent electrical circuit parameters.

Table A.1: NMC Li-ion battery equivalent circuit parameters

Electrical parameter	Value
R_0	0.1 - 3 Ω
R_1	0.5 Ω
C_1	300 F

Detailed explanations regarding the electrochemical impedance spectroscopy (EIS) technique, required to determine these parameters for NMC Li-ion cells are given in [26], [29].

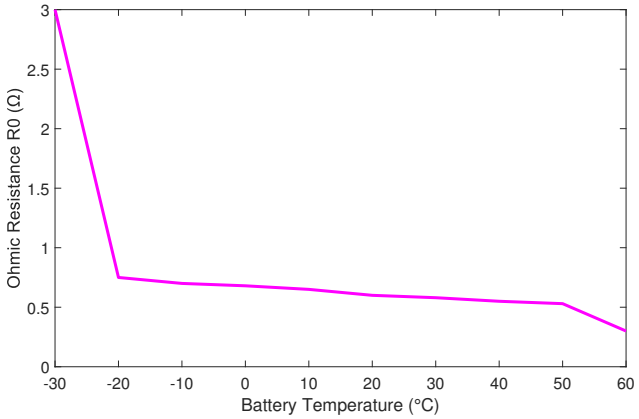

Figure A.3: Ohmic resistance (R_0) versus Battery Temperature

Figure A.3 shows the variation of the ohmic resistance R_0,with the battery temperature. It is called ohmic since it is the non-electrochemical resistance offered in the electrolyte, electrodes and current collector terminals.

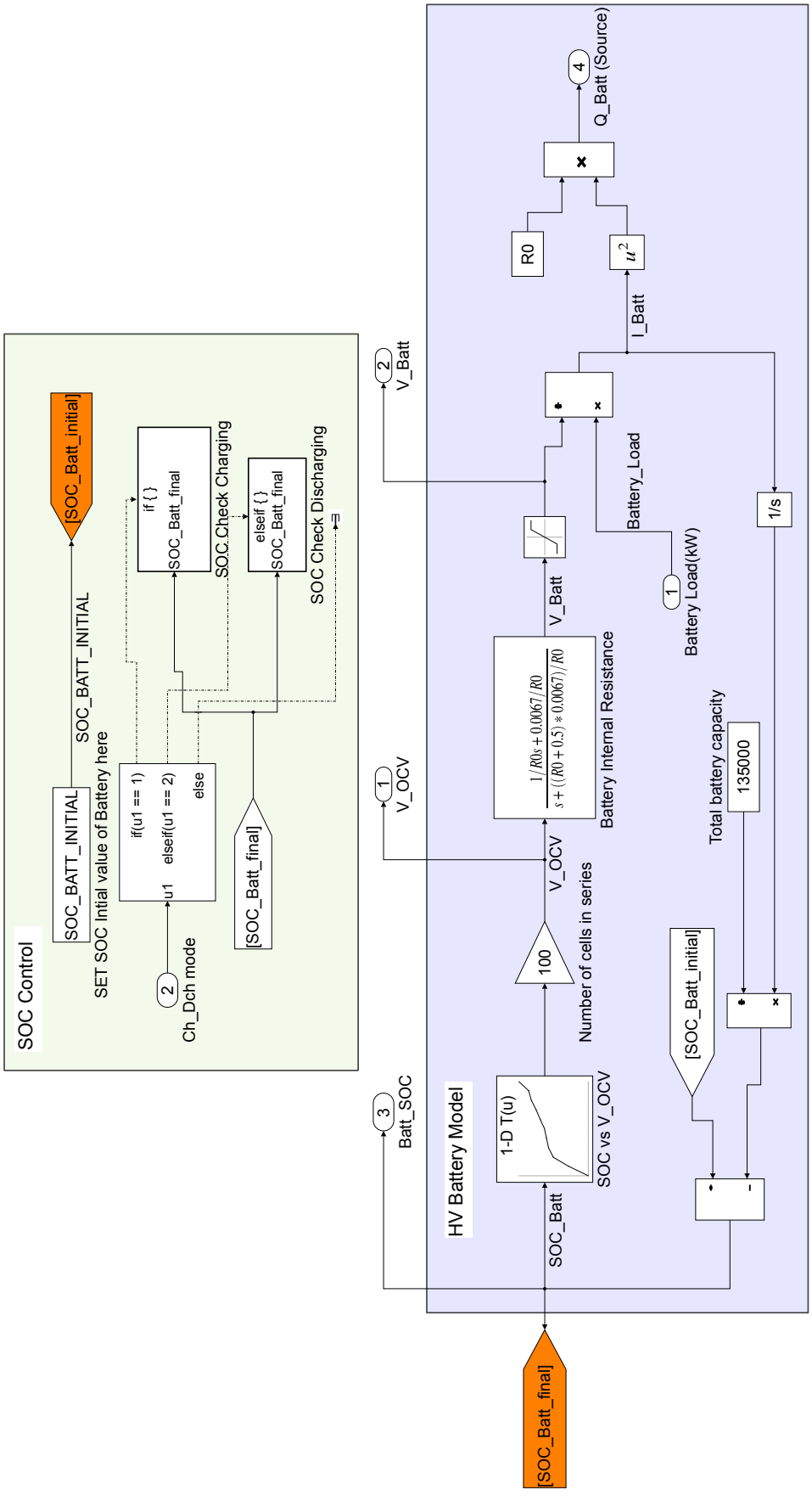

Figure A.4: HV battery electro-thermal model in Simulink

Figure A.4 shows the electro-thermal equivalent modelling of the battery in Simulink (MATLAB). The key objective is to model the battery internal resistance R_i as a function of Temperature and SOC. For a given load, the battery current is determined and then subsequently, the heat generated in the cells, $\dot{Q}_{source}$ could also be found out.

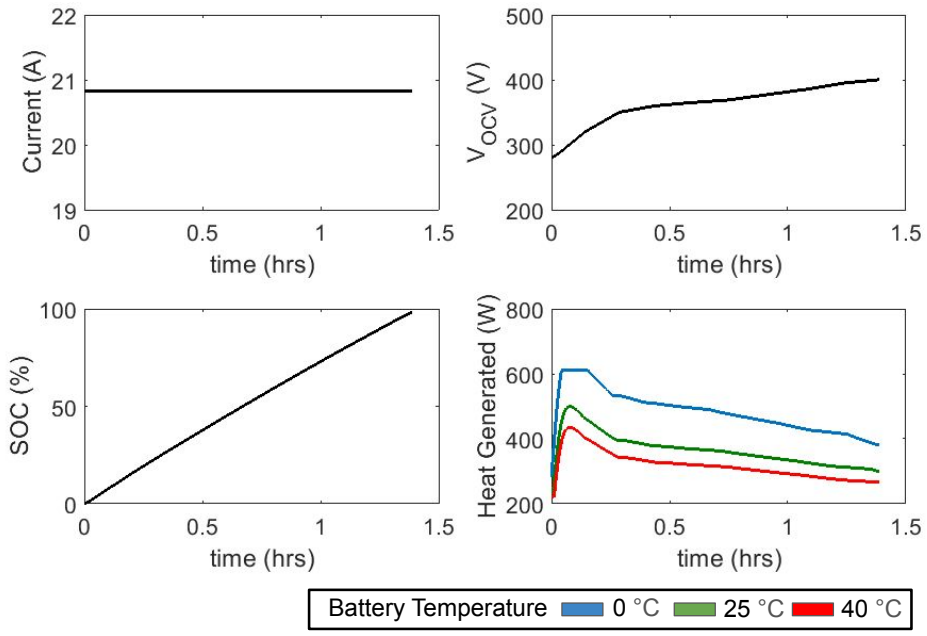

Figure A.5: HV battery simulation output

Figure A.5 shows the battery simulation results for a 50kW DC charging event. The simulation is repeated for ambient temperature conditions 0°C, 20°C, 40°C and the corresponding heat flux $\dot{Q}_{source}$, generated in the cells are obtained.

A.1.2 Calculation of lumped thermal network parameters

The heat generated in the cells are effectively carried to the cooling plate of the battery pack by conduction. Then the heat is removed using a coolant (ethylene glycol- water mixture or ambient air) by convection.

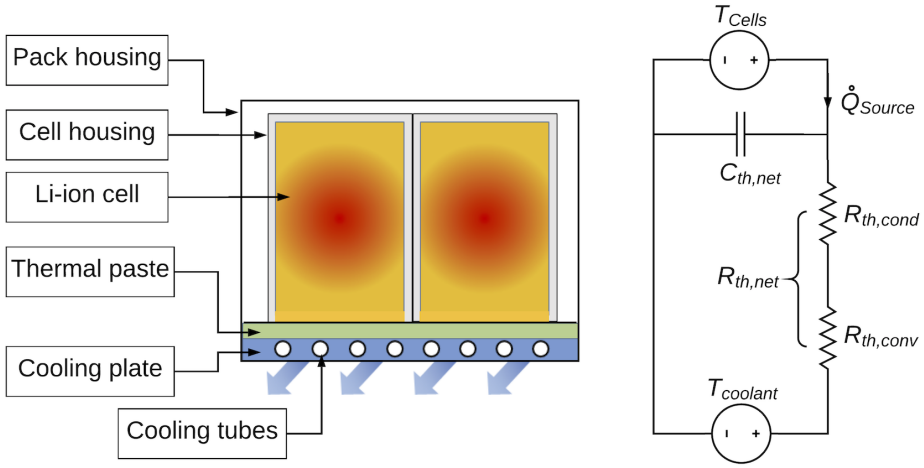

Figure A.6: Lumped thermal network of HV battery and its cooling system

The physical information about the cells and the battery required for conductive thermal resistance calculations is presented in Table A.2.

Table A.2: Physical parameters of the battery

Cell type	NMC Li-ion pouch
Cell dimension	(188*171*10.8)mm
Cell contact area(A)	(200*15)mm^2
Number of cells in series(N_{cells})	100
Thickness of thermal paste(d_1)	3.5 mm
Conductivity of thermal paste(λ_1)	6 W/mK
Thickness of cooling plate(d_2)	8 mm
Conductivity of cooling plate(λ_2)	239 W/mK

The thermal resistance along the conductive path from a cell to the cooling surface is given by,

$$R_{th,cond} = \frac{d_1}{\lambda_1 A} + \frac{d_2}{\lambda_2 A} \tag{A.1}$$

$$R_{th,cond} = 0.194K/W + 0.012K/W = 0.2K/W$$

Further calculating for the 100 cells which are electrically in series but, are separated by the cell housings and hence are thermally in parallel.

$$R_{th,cond} = \frac{0.2K/W}{N_{cells}} = 2K/kW$$

The information regarding the liquid coolant is presented in TableA.3.

Table A.3: Physical parameters of the liquid coolant

Coolant name	Ethylene glycol water
specific heat capacity(C_p)	$3340 J/kgK$
Flowrate of coolant	$6 LPM$
mass of coolant per sec ($\dot{m}$)	$0.1 kg/s$
Number of cooling tubes (N_{tubes})	8

The convective thermal resistance offered in one cooling tube due to the flowing coolant is given by,

$$R_{th,conv} = \frac{1}{\dot{m} C_p} \tag{A.2}$$

$$R_{th,conv} = 0.003 K/W$$

For 8 such cooling tubes, the net convective resistance would be,

$$R_{th,conv} = N_{tubes} * 0.003 K/W = 24 K/kW$$

When passive cooling is preferred instead, then the convection is due to the ambient air as coolant. The convective resistance now would depend upon the velocity of air across the cooling plate of the battery that is exposed to the ambient directly. This air velocity is directly dependent on the vehicle speed.

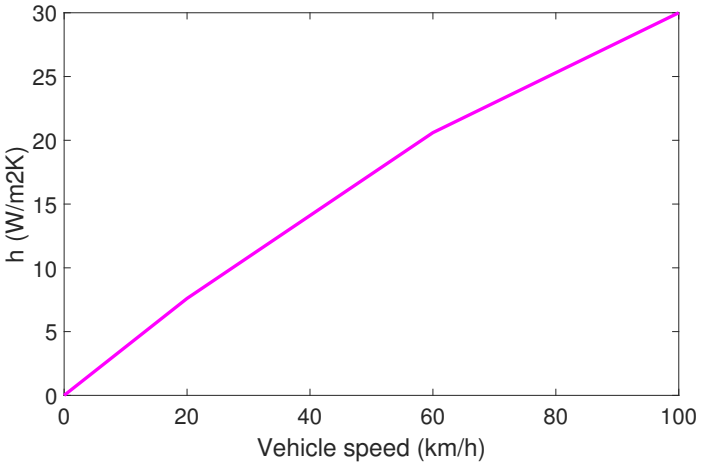

Figure A.7: Passive cooling convective heat transfer co-efficient versus vehicle speed

Figure A.7 shows the variation of convective heat transfer coefficient of air, h as a function of the vehicle speed. The data corresponding to the passively cooled battery used in this thesis is present in Table A.4

Table A.4: Physical parameters of the liquid coolant

Coolant name	Air
Heat transfer coefficient(h)	$10 W/m2K$
Battery pack dimension	(900*480*200)mm
Surface area of cooling plate(A)	900*480(mm^2)

$$R_{th,conv} = \frac{1}{hA} \tag{A.3}$$

$$R_{th,conv} = 0.231K/W = 231K/kW$$

The thermal resistance due to convection in a passively cooled battery is the value derived in (A.3). In this thesis, only a constant value heat transfer coeffcient, h is chosen. In future works, it maybe implemented further as a function of vehicle speed as shown in figure A.7.

A.1.3 Heat sinking using cooling system

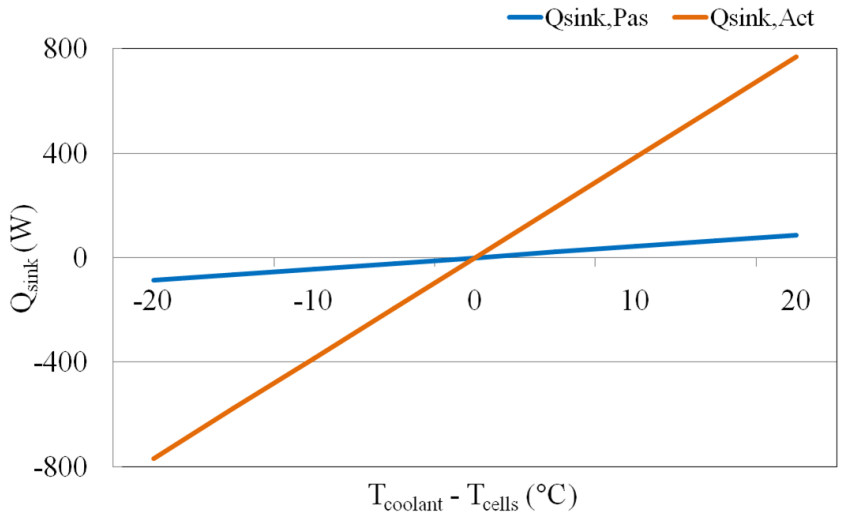

Figure A.8: Comparison of heat sinking for passive and active cooling systems

The y axis in fig.A.8, shows the $\dot{Q}_{sink}$ using the two cooling systems. The x axis is the temperature difference between the coolant and the cells. The coolant is ethyele glycol- water, mixture for active cooling system and air, for passive cooling system.

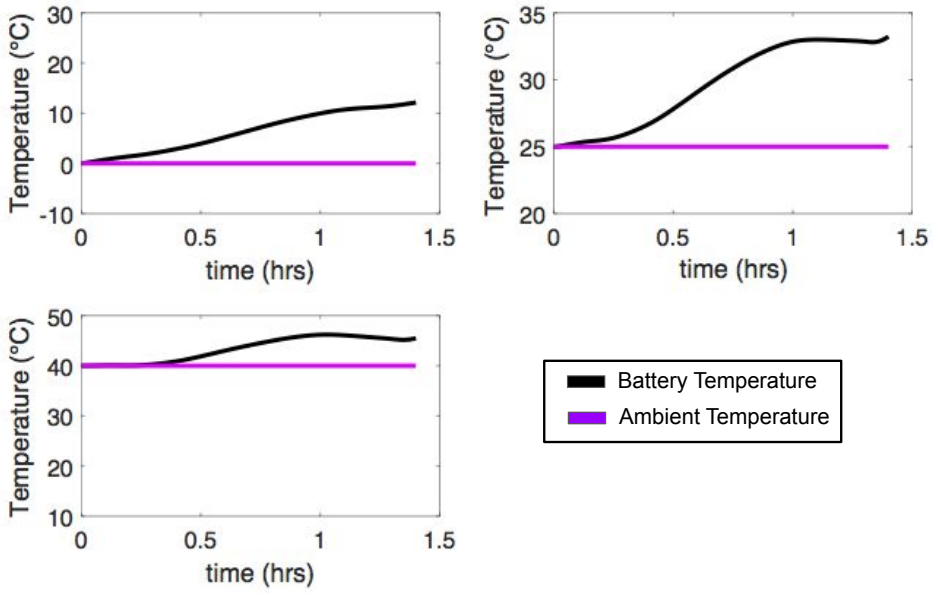

Figure A.9: Temperature profiles of passively cooled battery

The $\dot{Q}_{Source}$ generated in the cells during the constant current 50kW DC charging event for various ambient temperature conditions, produce temperature profiles for passively cooled battery as shown in the figure A.9.

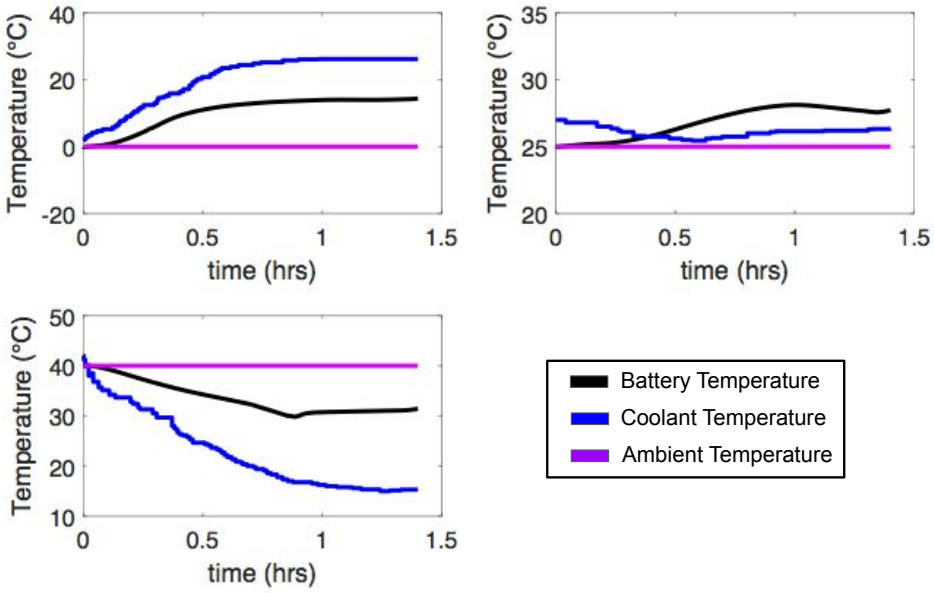

Figure A.10: Temperatrue profiles of actively cooled battery

Figure A.10, shows the ambient temperature, battery temperature and coolant output temperature for an actively cooled battery subjected to DC charging load.

B

Appendix 2

B.1 Performance and Feasibility comparisons for various market regions

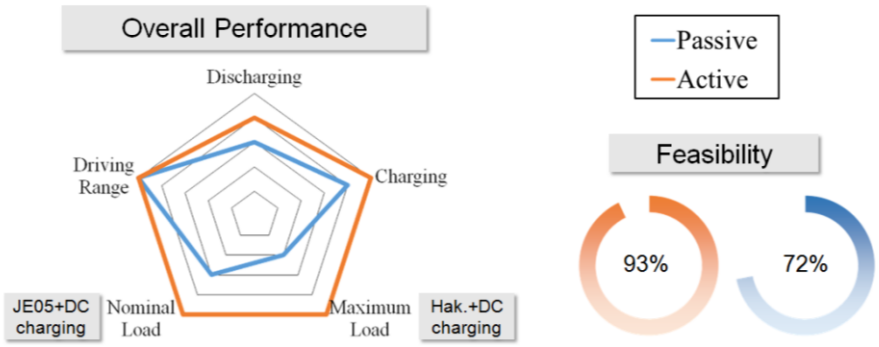

Figure B.1: Performance and feasibility of passively cooled batteries for Phoenix, AZ, USA

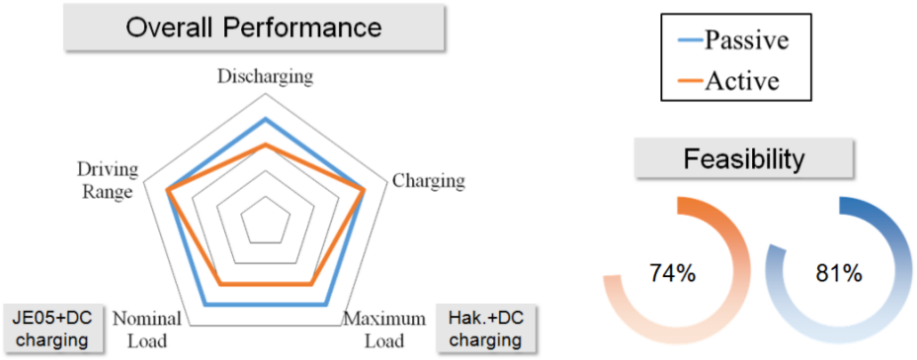

Figure B.2: Performance and feasibility of passively cooled batteries for Kiruna, Sweden

Figure B.3: Feasibility of HV battery cooling systems for various market regions

		Feasibility (100%)	
Market Regions	City	Actively cooled	Passively cooled
Europe	Madrid	85	82
	Malta	90	77
	Berlin	81	82
	Kiruna	74	81
	Helsinki	78	83
USA	Oregon	83	84
	California	91	80
	Phoenix	93	72
	Florida	96	75
	Northeast	85	81
	Illinois	84	82
Japan	Tokyo	88	80
	Sapporo	81	83
	Kumagaya	87	80